non-necrotic muscle fibers (2,3). These CD8 T cells express cytotoxic effector molecules, known as perforins, that are oriented toward target muscle fibers (4). Surface expression of class I major histocompatibility complex (MHC) molecules on muscle fibers is up-regulated (5). In a study of T cells from patients with PM compared with normal donors, CD8 T cell clones expanded more frequently in the peripheral blood of patients with PM (6,7). Moreover, some of these clones could be found in muscle biopsy samples from the same patients (6,7). All of these observations support the view that PM is driven by cytotoxic CD8 T cells.

In rheumatoid arthritis (RA), another autoimmune disease, biologic agents that block tumor necrosis factor α (TNFα) have been introduced into clinical use. TNFα blockade has an enormous effect in modulating the clinical course of RA (8). Animal models of arthritis serve to help identify therapeutic targets and to test the effect of these therapeutic reagents (9–11). In contrast, in PM, the lack of appropriate animal models has hampered basic research studies and delayed the development of new treatments.

Experimental autoimmune myositis (EAM), established previously as an animal model of PM, is inducible specifically in SJL/J mice by repeated administration of muscle homogenate or partially purified myosin (12,13). This model is a complex representation of disease, because SJL/J mice have a dysferlin gene mutation that causes spontaneous muscle necrosis and secondary muscle inflammation (14). Immunohistochemical studies have shown that infiltrating T cells in the muscle are dominated by CD4 T cells, suggesting that the EAM disease model is mediated by CD4 T cells (15).

We established a new murine model that can be induced with a single injection of a recombinant skeletal muscle fast-type C protein. This myosin-binding protein is in the cross-bridge–bearing zone of A bands of myofibrils (16,17). Biochemical purification studies showed that C protein appears to be the main immunopathogenic component of the crude skeletal-muscle myosin preparation used for the induction of experimental myositis in Lewis rats (18,19). In this study, we used recombinant protein fragments to confirm the immunogenicity of the C protein. This myositis, designated as C protein–induced myositis (CIM), can be induced in C57BL/6 (B6) mice and in other strains of mice. Its histologic and immunohistochemical features mimic those of PM. Functional studies have indicated that cytotoxic CD8 T cells are primarily responsible for the pathologic mechanisms of this disease.

Susceptibility to CIM in B6 mice has facilitated studies of the immunologic components required to induce myositis. In the present study, we were able to show that the effects of immunoglobulins are not necessary for the development of CIM, despite the presence of B cells in the affected muscles and anti–C protein antibodies in the sera. Although both interleukin-1 (IL-1)–positive and TNFα-positive cells infiltrated the muscles of affected mice, only IL-1, not TNFα, was crucial in the development of CIM. Interestingly, CIM was suppressed by infusion of intravenous immunoglobulins (IVIGs), which has been used as a last resort for treatment of patients with PM who do not respond to or tolerate immunosuppressive reagents. Thus, we show that our new model is useful in investigating the pathologic mechanisms of autoimmune myositis and in developing new treatment strategies for this disease.

MATERIALS AND METHODS

Mice. B6, SJL/J, BALB/c, DBA/1, and C3H/He mice were purchased from Charles River (Yokohama, Japan). NZB and MRL/Mp+/+ mice were purchased from SLC (Shizuoka, Japan). Mutant B6 mice rendered double-null for IL-1α/β were established previously (20), while Igμ-null mutant B6 mice (21) and TNFα-null mutant mice (22) were kindly provided by Drs. Karasuyama (Tokyo Medical and Dental University) and Sekikawa (formerly at the National Institute of Agrobiological Science), respectively. All experiments were done under specific pathogen–free conditions in accordance with the ethics and safety guidelines for animal experiments of Tokyo Medical and Dental University and RIKEN.

Recombinant human skeletal C protein. Four complementary DNA (cDNA) fragments encoding overlapping cDNA fragments 1, 2, 3, and 4 of human fast-type skeletal muscle C protein were amplified from human skeletal muscle cDNA using polymerase chain reaction. Primers used were 5′-GAGAGGTACCATGCCTGAGGCAAAACCAGCG-3′ and 5′-GAGAGTCGACTCAGAACCACTTGAGGGTCAGGTC-3′ for fragment 1, 5′-GAGAGGATCCGACCTGACCCTCAAGTGGTTC-3′ and 5′-GAGAAAGCTTTCACAGCCAGGTAGCGACGGGAGG-3′ for fragment 2, 5′-AGAGGATCCCCTCCCGTCGCTACCTGGCTG-3′ and 5′-GAGAAAGCTTTCACCGGGGCTTTCCCTGGAAGGG-3′ for fragment 3, and 5′-AGAGGATCCCCCTTCAGGGAAAGCCCCGG-3′ and 5′-GAGAAAGCTTTCACTGCGGCACTCGGACCTC-3′ for fragment 4 (Qiagen, Hilden, Germany) (underlining indicates the restriction enzyme recognition sites for subcloning into the pQE30 expression vector). These primers were introduced into the TOP10F′ bacterial host (Invitrogen, Carlsbad, CA) and were used to prepare recombinant C protein fragments according to the manufacturer's protocol. Soluble recombinant C proteins were dialyzed against 0.5*M* arginine, 2 m*M* reduced glutathione, 0.2 m*M* oxydized glutathione in phosphate buffered saline (PBS), pH 7.4 (fragments 1 and 2) or 25 m*M* glycine HCl, pH 3.0

(fragments 3 and 4). Endotoxin was removed using Detoxi-Gel Endotoxin Removal Gel (Pierce, Rockford, IL).

Induction of CIM. Female mice, ages 8–10 weeks, were immunized intradermally with 200 μg of the C protein fragments emulsified in Freund's complete adjuvant (CFA) containing 100 μg of heat-killed *Mycobacterium butyricum* (Difco, Detroit, MI). The immunogens were injected at multiple sites of the back and foot pads, and 2 μg of pertussis toxin (PT) (Seikagaku Kogyo, Tokyo, Japan) in PBS was injected intraperitoneally at the same time. Hematoxylin and eosin–stained 10-μm sections of the proximal muscles (hamstrings and quadriceps) were examined histologically for the presence of mononuclear cell infiltration and necrosis of muscle fibers. The histologic severity of inflammation in each muscle block was graded as follows (18,19): grade 1 = involvement of a single muscle fiber or <5 muscle fibers; grade 2 = a lesion involving 5–30 muscle fibers; grade 3 = a lesion involving a muscle fasciculus; and grade 4 = diffuse, extensive lesions. When multiple lesions with the same grade were found in a single muscle block, 0.5 point was added to the grade.

Immunohistochemical analysis. Cryostat-frozen sections (6 μm) fixed in cold acetone were stained with anti-CD8a (53-6.7; BD Biosciences PharMingen, San Diego, CA), anti-CD4 (H129.19; BD Biosciences PharMingen), anti-B220 (RA3-6B2; BD Biosciences PharMingen), anti-CD11b (M1/70; BD Biosciences PharMingen), anti-CD68 (FA-11; Serotec, Oxford, UK), anti–IL-1α (40508; Genzyme/Techne, Minneapolis, MN), or anti-TNFα (MP6-XT22; BioLegend, San Diego, CA) monoclonal antibodies (mAb). To stain perforin molecules, air-dried sections were treated with 0.5% periodic acid solution and then stained with antiperforin mAb (CB5.4; Alexis Biochemicals, San Diego, CA). Nonspecific staining was blocked with 4% Blockace (Dainippon, Osaka, Japan).

Bound antibodies were visualized with peroxidase-labeled anti-rat IgG antibodies and associated substrates (Histofine Simple Stain Max PO; Nichirei, Tokyo, Japan). The sections were also stained with biotinylated mouse anti-mouse H-2K^b mAb (AF6-88.5; BD Biosciences PharMingen) and with biotinylated mouse anti-mouse I-A^b mAb (AF6-120.1; BD Biosciences PharMingen). They were then incubated with peroxidase-conjugated streptavidin and its substrates (Chemicon, Temecula, CA). For double immunofluorescence staining, the sections were preincubated with 5% heat-inactivated rat serum and 1% bovine serum albumin, and were stained with Alexa Fluor 647–conjugated anti-CD8a mAb (53-6.7; BD Biosciences PharMingen) and fluorescein isothiocyanate (FITC)–conjugated anti-CD4 mAb (RM4-5; BD Biosciences PharMingen).

The bound antibodies were visualized using SP2AOBS confocal laser microscopy (Leica, Heidelberg, Germany). Spleens or popliteal lymph nodes were stained as positive controls. Isotype controls were used as negative control. The stained sections were evaluated by 2 independent observers, who reported results that were comparable.

Quantification of mononuclear cell subsets. The method used to quantify stained cells in the immunohistochemical analysis was based on a previously published method (2). Briefly, 5 inflammatory mononuclear cell foci in the serial sections from 4 mice with CIM were studied. At least 1 focus from each mouse was evaluated. Stained mononuclear cells infiltrating into the endomysial, perimysial, and perivascular sites of the foci were enumerated separately. The frequency of each subset was calculated in relation to the sum of all subsets. The CD4:CD8 ratios were calculated on the basis of these calculations. The CD4:CD8 ratios in double immunofluorescence staining were calculated in the same manner as in the immunohistochemical analyses. CD68-positive and CD11b-positive cells in the serial sections were also enumerated in the same manner, and the frequencies of CD68-positive cells were calculated in relation to the number of CD11b-positive cells.

Rotarod test. Muscle function was evaluated with a MK-630 rotarod device (Muromachi Kikai, Tokyo, Japan) as described previously (23). The rotarod test was performed on each mouse by measuring the running time until the mouse fell off the rod while the rod was turning at 20 revolutions per minute for 200 seconds. The running ability of each mouse was scored in 5 categories of running time: score 1 = 0–49 seconds, score 2 = 50–99 seconds, score 3 = 100–149 seconds, score 4 = 150–200 seconds, score 5 = >200 seconds. Mice were initially trained to accommodate them to the task, and then tested 2 days thereafter.

In vivo depletion of CD8 or CD4 T cells. For the depletion of CD8 or CD4 T cells in B6 mice, the mice were injected intraperitoneally with 1 mg of purified anti-CD8 (53.67.2) mAb (24), anti-CD4 (GK1.5) mAb (24), or purified rat IgG (Sigma-Aldrich, St. Louis, MO) as a control, for 3 consecutive days. This treatment started 10 days before the immunization. Injection of 500 μg of the same mAb was repeated every other day for 14 days. Splenocytes and lymph node cells from the treated mice were stained with phycoerythrin (PE)–conjugated anti-CD8 mAb (53.67; BD Biosciences PharMingen) or PE-conjugated anti-CD4 mAb (H129.19; BD Biosciences PharMingen), together with FITC-conjugated anti-CD3 mAb (145-2C11; BD Biosciences PharMingen). The cells were then analyzed with FACSCalibur (Becton Dickinson, San Jose, CA).

IVIG treatment. A subgroup of the mice were treated with IVIG. Human gamma immunoglobulins (Venoglobulin-IH; Benesis, Osaka, Japan) (400 mg/kg/day) were injected intravenously into the tail vein for 5 consecutive days, beginning 3 days after immunization.

Statistical analysis. Histologic scores were compared with the Mann-Whitney U test. *P* values less than or equal to 0.05 were considered significant.

RESULTS

Histologic features of CIM in immunized mice. Recombinant human fast-type skeletal C protein fragments were prepared using a prokaryotic expression system. Because of the size of the C protein, 4 overlapping protein fragments were generated: fragment 1 (amino acids 1–290), fragment 2 (amino acids 284–580), fragment 3 (amino acids 567–877), and fragment 4 (amino acids 864–1142). B6 mice were immunized at multiple sites of the back and foot pads with each fragment emulsified in CFA. PT was also injected intraperitoneally. To compare the immunogenicity of the 4 fragments, 5 mice per group were immunized with each

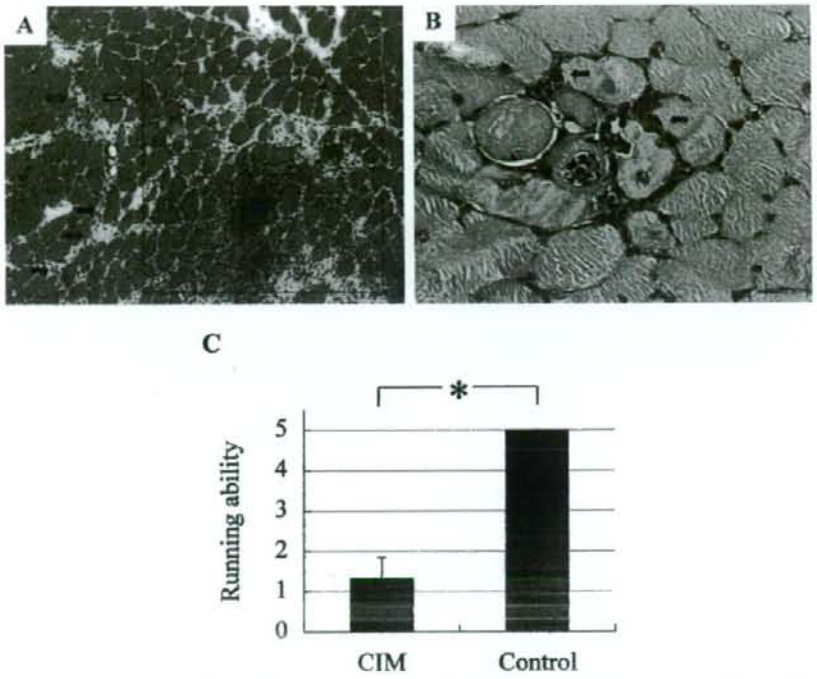

Figure 1. Muscle inflammation in C protein–induced myositis (CIM). C57BL/6 mice were immunized once with recombinant human skeletal C protein fragment 2 to induce CIM. **A** and **B,** Mononuclear cell infiltration was found predominantly in the endomysial site (boxed area) but also in the perimysial site (**solid arrows**) and perivascular site (**open arrows**) (**A**). Many cells invaded non-necrotic muscle fibers (**arrows**), while necrotic fibers were also present (**B**). Bar in **A** = 100 μm; bar in **B** = 25 μm. **C,** Muscle function was evaluated with a rotarod test 21 days after immunization. Six mice with CIM and 5 control mice treated with adjuvant alone were examined. Running ability was scored as described in Materials and Methods. Values are the mean and SD score. * = $P < 0.01$.

fragment, and myositis was studied histologically 21 days after the immunizaton.

None of the mice treated with adjuvant alone or immunized without PT developed myositis. We found that a single immunization of fragments 2 or 4 induced myositis consistently, and the mean ± SD histologic scores were 2.8 ± 0.2 and 1.0 ± 0.3, respectively. Fragments 1 and 3 induced milder myositis at a lower incidence, and the mean ± SD histologic scores were 0.2 ± 0.3 and 0.1 ± 0.2, respectively. Because fragment 2 induced the most severe myositis, it was used as an immunogen in subsequent experiments.

Histologic analysis of the muscles affected by CIM showed that mononuclear cells infiltrated predominantly the endomysial site, but also the perimysial and perivascular sites of the muscle tissue (Figure 1A). Many mononuclear cells invaded non-necrotic muscle fibers (Figure 1B). No abnormality in cardiac muscle and other tissues, including lung and joint tissues, was observed. Muscle function was assessed clinically with a rotarod device on day 21. Consistent with the histologic findings in the muscle tissue, mice with CIM ran for a shorter time than did control mice, indicating a reduction in motor function (Figure 1C).

Inflammation is acute and regresses spontaneously in most animal models of autoimmune diseases. To study the course of CIM in mice, muscle sections from 4 or 5 mice were examined at various time points after the immunization. A small number of mononuclear cells appeared in 50% of the muscle samples on day 7

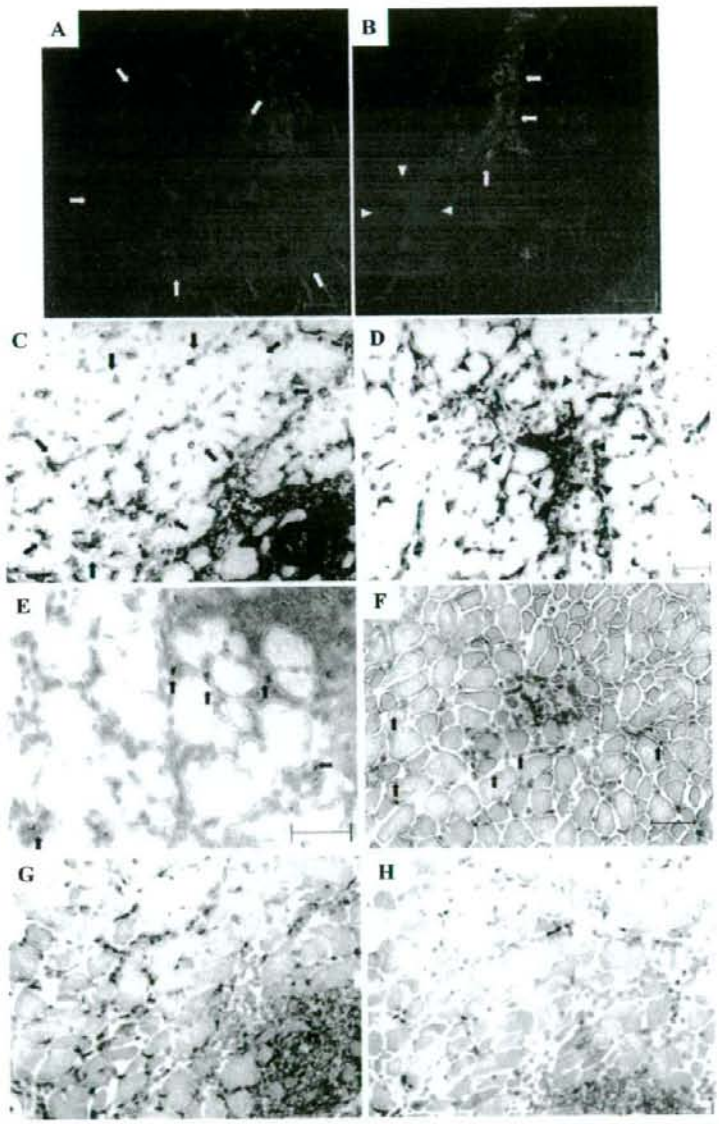

Figure 2. Immunohistochemical findings in muscles of mice with C protein–induced myositis. **A** and **B,** Expression of CD4 (green, fluorescein isothiocyanate) and CD8 (red, Alexa Fluor 647) was examined. Infiltrating cells in the endomysial site (**arrows**) (**A**) and in the perimysial site (**arrows**) and perivascular site (**arrowheads**) (**B**) were individually enumerated for calculating CD4:CD8 ratios. **C–H,** Expression of CD11b (**C** and **D**), perforin (**E**), class I major histocompatibility complex (**F**), interleukin-1α (IL-1α) (**G**), and tumor necrosis factor α (TNFα) (**H**) was examined with immunoperoxidase staining. CD11b-positive cells diffusely infiltrated the endomysial site (**arrows**) (**C**) and both the perimysial (**arrows**) and perivascular sites (**arrowheads**) (**D**). Perforin-positive cells infiltrated around non-necrotic muscle fibers at the endomysial sites (**arrows**) (**E**). Muscle fibers reacted to anti-$H2K^b$ monoclonal antibodies (**arrows**) (**F**). IL-1α and TNFα were expressed on infiltrating mononuclear cells in muscles (**G** and **H**). Bars = 50 μm.

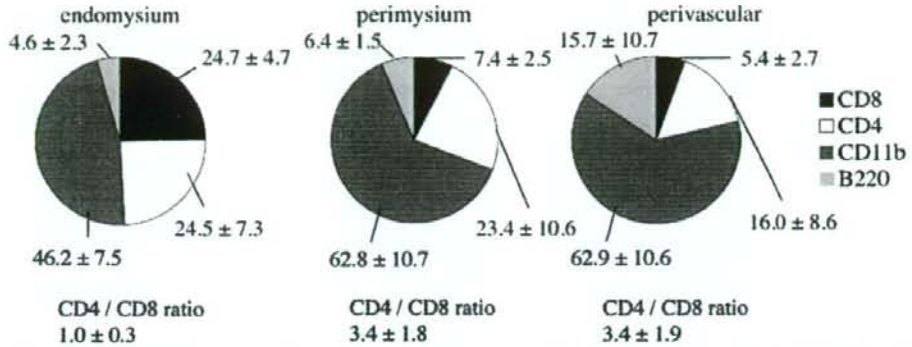

Figure 3. Quantitative immunohistochemical analysis of mononuclear cells in muscles of mice with C protein–induced myositis. Frequencies of CD8, CD4, CD11b, and B220 cells in the infiltrating mononuclear cells at endomysial, perimysial, and perivascular sites are shown. Values are the mean ± SD percentage of each cell subset and mean ± SD CD4:CD8 ratio at 5 inflammatory mononuclear cell foci. The total mononuclear cell counts in the endomysial, perimysial, and perivascular sites were 1,385, 506, and 543, respectively.

(incidence 50%, mean ± SD histologic score 0.6 ± 0.7). Inflammation of the muscle tissue peaked on days 14 and 21 after the immunization (incidence 100%, histologic scores 2.6 ± 0.3 and 2.8 ± 0.2, respectively) and started to resolve after day 28 (incidence 100%, histologic score 1.4 ± 0.6). On day 49, mononuclear cell infiltration was absent from most skeletal muscles. On days 35, 49, and 63, the histologic scores were 0.5 ± 0.6, 0.1 ± 0.2, and 0.0 ± 0.0, respectively, and the incidences of CIM were 38%, 10%, and 0%, respectively.

Other strains of mice were immunized with fragment 2 of the C protein in the same manner as in B6 mice, and the muscles were examined histologically. Studies of 4 or 5 mice per strain showed that myositis developed in NZB and SJL/J mice with an incidence similar to that in B6 mice. However, the mononuclear cell infiltration was less intense. The mean ± SD histologic scores were 1.8 ± 0.6 and 1.3 ± 0.3 in NZB and SJL/J mice, respectively. No inflammation was observed in the muscles from BALB/c, DBA/1, C3H/He, or MRL/Mp+/+ mice immunized with C protein fragments.

Immunohistochemical findings in muscles of mice with CIM. Localization of CD4 and CD8 T cells was studied with double immnunofluorescence labeling or immunohistochemical staining of muscle sections. CD4 cells diffusely infiltrated the endomysial, perimysial, and perivascular sites. In contrast, CD8 cells infiltrated preferentially the endomysial site (Figures 2A and B), which was reflected equally well in the CD4:CD8 cell ratios. Double immnunofluorescence staining of CD4 and CD8 cells showed that the mean ± SD CD4:CD8 ratios in the endomysium, perimysium, and perivascular site were 1.0 ± 0.1, 3.3 ± 0.3, and 3.5 ± 0.4, respectively, which was consistent with the ratios derived from immunohistochemical staining (Figure 3). The frequency of CD8-positive cells in endomysial sites was higher than that in perimysial and perivascular sites, whereas the frequencies of CD4-positive T cells were similar among the 3 sites (Figure 3).

B cells and macrophages were identified by staining with B220 and CD11b antibodies, respectively. CD11b-positive cells were most abundant among the infiltrating cells in all 3 sites (Figures 2C and D and Figure 3). Although natural killer cells are also CD11b positive, our analysis of CD68 and CD11b expression in serial sections showed that 93.4 ± 4.3% (mean ± SD) of CD11b-positive cells were CD68-positive cells, indicating that the majority of CD11b-positive cells were macrophages.

B cells were sparse in the muscle tissue, especially in the endomysial and perimysial sites (Figure 3). Perforin-positive cells were present mostly (82%) around non-necrotic muscle fibers at the endomysial site (Figure 2E) and were sparse in the perimysial and perivascular sites (results not shown). Thus, the distribution of perforin-positive cells corresponded well to that of CD8-positive cells. When muscle fibers were stained with anti-H2K^b (class I MHC) and anti–I-A^b (class II MHC) mAb, they reacted to the anti–class I

MHC mAb (Figure 2F) but not to the anti–class II MHC mAb (results not shown).

Pathologic role of CD8 and CD4 T cells in CIM. Histologic studies have demonstrated that CD8 T cells function as effector cells in injury of muscle fibers. To establish the pathologic role of CD8 T cells, B6 mice were pretreated by removal of circulating CD8 T cells using specific mAb. Ten days after injection of the antibodies for 3 consecutive days, CD8 T cells in the spleens were depleted to fewer than 2%. The mice were then immunized with C protein and treated with the same antibodies every other day for 14 days. The muscles were examined histologically 14 days after the immunization, when the frequency of CD8 T cells in the spleens and lymph nodes was still less than 2%. The number of CD4 T cells in the spleens and lymph nodes was maintained in the CD8-depleted mice.

Significantly fewer CD8-depleted mice developed myositis compared with control mice, with a 33% incidence of disease compared with 100% in controls (Table 1). The histologic scores of the treated mice were significantly lower than that of the controls. It is known that CD4 T cells help CD8 T cells develop into mature cytotoxic T lymphocytes. They also have the potential to injure muscle fibers. Therefore, CD4 T cells were removed with specific mAb in the same manner as described above for CD8 T cells. The pretreated mice exhibited fewer than 2% of circulating CD4 T cells, and were then immunized for CIM induction. They also developed a milder myositis compared with control mice (Table 1).

Investigation of essential immunologic mediators in mutant mice. Mice with CIM developed serum antibodies directed to C protein. They also developed low-titer autoantibodies with a cytoplasmic pattern or homogeneous and speckled nuclear patterns on Hep-2 staining, which proved to be nonreactive to PM-associated autoantigens (results not shown). However, the contribution of these autoantibodies to myositis was unclear.

The susceptibility of B6 mice to CIM allowed us to study the contribution of different immune mediators to myositis using genetic mutant mice. Igμ-null mutant mice developed CIM with features and a frequency comparable with those in control wild-type (WT) mice (Table 1). These findings indicate that the functions of B cells and immunoglobulins are not necessary for the development of CIM.

Inflammatory cytokines such as IL-1 and TNFα are known to be expressed in mononuclear cells infiltrating the muscles of mice with PM (25,26). Our immunohistochemical analyses showed that these inflammatory cytokines were also found in mice with CIM (Figures 2G and H). We then studied whether the presence of IL-1 and TNFα is required for the development of CIM, using IL-1α/β double-null mutant and TNFα-null mutant B6 mice. Most IL-1α/β–null mutant mice did not develop myositis, and those that did have myositis developed a mild form (Table 1). The rotarod score of 7 for the IL-1α/β–null mutant mice was significantly higher than that for the 6 WT mice (mean ± SD score 4.7 ± 0.5 versus 1.3 ± 0.5; $P < 0.01$). In contrast, TNFα-null mutant mice were as susceptible to CIM as the control mice, and the TNFα-null mice had a similar incidence and severity of myositis (Table 1). These results indicate the differential requirements for the roles of IL-1 and TNFα in the development of CIM.

Table 1. Studies of the pathologic features of C protein–induced polymyositis (CIM) and effects of treatment with intravenous immunoglobulin (IVIG)*

Experiment, mouse group	Incidence of CIM, %	Muscle blocks involved, %†	Histologic score, mean ± SD
CD8 depletion			
CD8-depleted	33	25	0.6 ± 1.0‡
Rat IgG–injected	100	100	1.9 ± 0.6
CD4 depletion			
CD4-depleted	60	50	0.7 ± 0.7‡
Rat IgG–injected	100	100	2.0 ± 0.4
Igμ-null			
Ig$\mu^{-/-}$	100	95	1.7 ± 0.6
WT	100	100	2.1 ± 0.7
IL-1-null			
IL-1$\alpha/\beta^{-/-}$	14	7	0.1 ± 0.2§
WT	100	100	2.1 ± 0.5
TNFα-null			
TNF$\alpha^{-/-}$	80	80	1.9 ± 1.0
WT	100	90	2.3 ± 0.6
IVIG			
IVIG-injected	43	36	0.6 ± 1.1‡
Saline-injected	100	100	2.3 ± 1.0

* Mice were immunized with 200 μg of the recombinant C protein fragments and then examined histologically 14 or 21 days after immunization. For in vivo depletion of CD8 or CD4 T cells, 5 or 6 B6 mice were treated intraperitoneally with anti-CD8 or anti-CD4 monoclonal antibodies, while 5 or 6 control mice were treated with purified rat IgG. To demonstrate the requirement for humoral immunity, the presence of interleukin-1 (IL-1), and the presence of tumor necrosis factor α (TNFα) for the development of CIM, 5 Igμ-null mutant mice, 7 IL-1α/β–null mutant mice, 5 TNFα-null mutant mice, and 5 wild-type (WT) B6 mice were studied. IVIG was administered at a dosage of 400 mg/kg/day intravenously into the tail vein for 5 consecutive days, from day 3 after immunization. Seven mice were treated with IVIG and 6 with control saline.

† Calculated as the number of muscle blocks showing myositis divided by the total number of blocks.

‡ $P < 0.05$ versus control group.

§ $P < 0.01$ versus control group.

Effects of high-dose IVIG treatment. Infusion of high-dose IVIG is effective treatment of inflammatory myopathies that are refractory to conventional immunosuppressants (27–29). Although several mechanisms of action for IVIG have been proposed, they have not been fully characterized. One possibility is that IVIG acts via suppression of pathogenic immunoglobulins and B cells. Thus, whether this treatment improves CIM, which does not depend on humoral immunity for tissue injury, is of special interest. When mice with CIM were treated with high-dose IVIG (400 mg/kg) for 5 consecutive days, beginning 3 days after immunization, the incidence and histologic severity of CIM were suppressed significantly compared with that in control, saline-injected mice (Table 1).

DISCUSSION

CIM was established as a simple murine model of PM. A single injection of mice with recombinant human muscle protein induced severe and clinically significant inflammation of the skeletal muscles. CD8 T cells were enriched in the endomysial site (the site of muscle injury) as compared with their distribution in other sites of the mouse muscle. CD8 cells expressed perforins preferentially at the endomysial site. Class I MHC expression was up-regulated on the muscle fibers. Removal of CD8 T cells significantly suppressed myositis. Thus, muscle injury in CIM appears to be driven, primarily, by cytotoxic CD8 T cells, as is assumed in human PM. In this regard, the new model provides a clear contrast to the previous EAM model, which appears to be driven by CD4 T cells. Induction of EAM requires repeated immunization with a specific mouse strain having a dysferlin gene mutation that induces spontaneous muscular degeneration and inflammation. Sensitivity of B6 mice to CIM prompted the initiation of genetic studies of the pathologic mechanisms of autoimmune myositis, which would provide information for the development of new treatments.

Muscle tissues from mice with CIM contained more CD4 T cells and macrophages than are found in patients with PM, which may reflect the acute disease course of CIM. Although we observed critical participation by CD8 T cells, CD4 T cells were also important in the development of CIM. In this regard, it has been shown that the actions of CD4 T cells are essential for full differentiation of cytotoxic CD8 T cells (30,31). Alternatively, CD4 T cells may also injure muscle tissues directly. This issue should be addressed further in future experiments.

Severe inflammation was found consistently in the proximal muscles of the lower extremities, but not in other sites. Although injection of CFA alone did not induce myositis, we assume that activation of local innate immunity by injection of the foot pad with CFA would contribute to induction of severe myositis. Unlike inflammation in human PM, inflammation in other myositis models, such as EAM and cardiac myosin–induced myocarditis, is transient (32,33). Because lipopolysaccharide injection in the recovery phase of experimental myocarditis can induce a relapse of inflammation (33), unknown factors might perpetuate the chronic disease in humans.

An elevation in the levels of creatine kinase (CK) was found in the mice with CIM. However, since some mice, including healthy animals, have unexpectedly high levels of CK, this elevation could be attributed to uncontrollable hemolysis. Lung involvement in some patients is characteristic of PM and also of dermatomyositis (DM). However, no abnormality in the lungs was observed in the mice with CIM. Considering the frequency of lung disease in PM (34), we may have to undertake extensive studies of this issue using a large number of animals.

Recombinant C protein was used to confirm its immunogenicity, as suggested in a rat myositis model induced by biochemically purified C protein (19). Large-scale production of recombinant C protein fragments in the prokaryotic expression system facilitated multiple experiments to optimize an immunization protocol and to analyze the pathologic features of myositis. Since at least 200 μg of the immunogen had to be injected to induce CIM consistently, we needed to use the back and foot pads of the mice for immunization.

The rotarod test was useful to assess muscle function in the mice with CIM at a single time point. Analysis by Spearman's rank correlation coefficient showed that the rotarod score correlated well with the histologic score ($P < 0.001$). However, this test was less useful in evaluating the disease course in these mice, because the mice could learn how to run for a longer period of time when the test was repeated. We believe that the device should be improved so that muscle function or weakness can be evaluated in an easier way.

Unlike in the EAM model, many strains of mice, including SJL/J mice, were susceptible to CIM. This fact confirms the immunogenicity of the C protein and suggests that mouse strains may have their own hierarchy of susceptibility to myositis.

Our observations of CIM induced in the B6 mice with mutations in inflammatory cytokine genes demon-

strated the importance of IL-1, but not TNFα, in the development of myositis. Previous histologic studies of PM muscle tissue showed that IL-1 and other proinflammatory cytokines, including TNFα, IL-6, and interferon-γ, are expressed by mononuclear cells in the affected muscle tissue (25). IL-1 expression by mononuclear cells accompanies expression of class I MHC molecules on the muscle fibers and expression of adhesion molecules, such as intercellular adhesion molecule 1 and vascular cell adhesion molecule 1, on endothelial cells in muscle (35). Thus, we assume that IL-1 expression of activated macrophages up-regulates expression of the class I MHC molecules, as well as that of adhesion molecules and chemokines, on muscle fibers, endothelial cells, and inflammatory cells. All of these molecules can trigger CD8-mediated muscle damage. Other studies have shown that antigen-specific T cell responses are impaired in IL-1α/β double-null mutant mice (36,37). In the autoimmune myocarditis model, IL-1 is important for efficient activation of dendritic cells (DCs) and priming of CD4 T cells (38). IL-1 may also contribute to activation of DCs and interacting T lymphocytes.

Similar to IL-1, TNFα induces expression of class I MHC molecules on muscle fibers and expression of adhesion molecules on endothelial cells (39,40). The results of one report suggested that TNFα released from infiltrating CD8 T cells in PM muscles was responsible for the muscle damage (26). However, we found that CD8 T cells can induce typical myositis without TNFα. In this regard, experimental myocarditis is suppressed in both IL-1 receptor– and TNFα receptor–null mutant mice (38,41), and this model is mediated by pathogenic CD4 T cells (33,38). Thus, it is important to note the differences between the 2 murine myositis models.

Our results do not necessarily refute the idea that TNFα is a therapeutic target in PM. Clinical findings from sporadic reports suggest that some patients with PM respond to systemic delivery of anti-TNFα mAb (42). This fact and our results are similar to the findings in collagen-induced arthritis (CIA), which is an animal model of RA. TNFα-null mutant mice are susceptible to CIA (43), but inhibition of TNFα can improve the disease (9). Development of arthritis is suppressed in IL-1α/β double-null mutant mice (37). Studies are in progress to investigate the therapeutic effects of IL-1 or TNFα blockade in CIM.

A high dose of IVIGs, pooled from the plasma of healthy donors, is commonly administered as treatment in patients with autoimmune disorders (44). After an initial study showing that a patient with refractory PM was successfully treated with IVIG (29), the efficacy has been confirmed by a number of studies of patients with PM and DM (27,28). Currently, IVIG therapy is the only treatment that does not induce general immune suppression. The same treatment exerted a minor therapeutic effect in SJL/J mice in the myositis model (45). Although immunoglobulins are derived from human sera, the effect was not due to nonspecific immunomodulation by a xenogenic protein.

We found that IVIG treatment was markedly effective in CIM, suggesting its relevance as a model for human PM. When the treatment was started 8 days after immunization of the mice, the therapeutic effect appeared milder (results not shown). The mode of action of IVIGs could vary, and all of the mechanisms have not been fully characterized (46–48). Modulation of crystallizable fragment Fcγ receptor IIb on phagocytes appears to be the primary mechanism for an increase in platelet counts in patients with immune thrombocytopenia (49). Theoretically, the treatment could also down-regulate activating Fcγ receptors, increase IgG catabolism, neutralize autoantibodies and inflammatory cytokines, attenuate complement-mediated tissue damage, and modulate cytokine production by B cells and monocytes. Because development of CIM does not depend on B cells or antibodies, the efficacy of IVIG treatment for this model suggests that down-regulation of B cells or autoantibody-mediated processes are not a prerequisite to achieve improvement of PM. Further evaluation should lead to identification of key molecules for the effect of IVIG and development of new treatments that target defined molecules.

Our new model mimics human PM and provides a useful tool to investigate its pathologic mechanisms. It holds promise for identification of specific targets that will lead to the development of new therapeutic approaches in the treatment of PM, and will also be useful for confirming the efficacy of these treatments.

ACKNOWLEDGMENTS

We thank H. Karasuyama for providing the Igμ-null mutant mice, K. Sekikawa for the TNFα-null mutant mice, M. Azuma for the hybridoma-producing anti-CD8 (53.67.2) mAb, A. Suwa and T. Mimori for performing the detection of autoantibodies, and E. Hirasawa for her critical advice.

AUTHOR CONTRIBUTIONS

Dr. Kohsaka had full access to all of the data in the study and takes responsibility for the integrity of the data and the accuracy of the data analysis.

Study design. Sugihara, Kohsaka.

Acquisition of data. Sugihara, Sekine, Nakae, Kohyama.

Analysis and interpretation of data. Sugihara, Harigai, Iwakura, Matsumoto, Miyasaka, Kohsaka.
Manuscript preparation. Sugihara, Kohsaka.
Statistical analysis. Sugihara, Kohsaka.

REFERENCES

1. Dalakas MC, Hohlfeld R. Polymyositis and dermatomyositis. Lancet 2003;362:971–82.
2. Arahata K, Engel AG. Monoclonal antibody analysis of mononuclear cells in myopathies. I. Quantitation of subsets according to diagnosis and sites of accumulation and demonstration and counts of muscle fibers invaded by T cells. Ann Neurol 1984;16:193–208.
3. Engel AG, Arahata K. Monoclonal antibody analysis of mononuclear cells in myopathies. II. Phenotypes of autoinvasive cells in polymyositis and inclusion body myositis. Ann Neurol 1984;16: 209–15.
4. Goebels N, Michaelis D, Engelhardt M, Huber S, Bender A, Pongratz D, et al. Differential expression of perforin in muscle-infiltrating T cells in polymyositis and dermatomyositis. J Clin Invest 1996;97:2905–10.
5. Emslie-Smith AM, Arahata K, Engel AG. Major histocompatibility complex class I antigen expression, immunolocalization of interferon subtypes, and T cell-mediated cytotoxicity in myopathies. Hum Pathol 1989;20:224–31.
6. Bender A, Ernst N, Iglesias A, Dornmair K, Wekerle H, Hohlfeld R. T cell receptor repertoire in polymyositis: clonal expansion of autoaggressive CD8+ T cells. J Exp Med 1995;181:1863–8.
7. Nishio J, Suzuki M, Miyasaka N, Kohsaka H. Clonal biases of peripheral CD8 T cell repertoire directly reflect local inflammation in polymyositis. J Immunol 2001;167:4051–8.
8. Lipsky PE, van der Heijde DM, St.Clair EW, Furst DE, Breedveld FC, Kalden JR, et al, for the Anti–Tumor Necrosis Factor Trial in Rheumatoid Arthritis with Concomitant Therapy Study Group. Infliximab and methotrexate in the treatment of rheumatoid arthritis. N Engl J Med 2000;343:1594–602.
9. Williams RO, Feldmann M, Maini RN. Anti-tumor necrosis factor ameliorates joint disease in murine collagen-induced arthritis. Proc Natl Acad Sci U S A 1992;89:9784–8.
10. Takagi N, Mihara M, Moriya Y, Nishimoto N, Yoshizaki K, Kishimoto T, et al. Blockage of interleukin-6 receptor ameliorates joint disease in murine collagen-induced arthritis. Arthritis Rheum 1998;41:2117–21.
11. Taniguchi K, Kohsaka H, Inoue N, Terada Y, Ito H, Hirokawa K, et al. Induction of the p16INK4a senescence gene as a new therapeutic strategy for the treatment of rheumatoid arthritis. Nat Med 1999;7:760–7.
12. Rosenberg NL, Ringel SP, Kotzin BL. Experimental autoimmune myositis in SJL/J mice. Clin Exp Immunol 1987;68:117–29.
13. Matsubara S, Shima T, Takamori M. Experimental allergic myositis in SJL/J mice immunized with rabbit myosin B fraction: immunohistochemical analysis and transfer. Acta Neuropathol (Berl) 1993;85:138–44.
14. Bittner RE, Anderson LV, Burkhardt E, Bashir R, Vafiadaki E, Ivanova S, et al. Dysferlin deletion in SJL mice (SJL-Dysf) defines a natural model for limb girdle muscular dystrophy 2B. Nat Genet 1999;23:141–2.
15. Rosenberg NL, Kotzin BL. Aberrant expression of class II MHC antigens by skeletal muscle endothelial cells in experimental autoimmune myositis. J Immunol 1989;142:4289–94.
16. Weber FE, Vaughan KT, Reinach FC, Fischman DA. Complete sequence of human fast-type and slow-type muscle myosin-binding-protein C (MyBP-C): differential expression, conserved domain structure and chromosome assignment. Eur J Biochem 1993;216:661–9.
17. Gilbert R, Cohen JA, Pardo S, Basu A, Fischman DA. Identification of the A-band localization domain of myosin binding proteins C and H (MyBP-C, MyBP-H) in skeletal muscle. J Cell Sci 1999;112:69–79.
18. Kojima T, Tanuma N, Aikawa Y, Shin T, Sasaki A, Matsumoto Y. Myosin-induced autoimmune polymyositis in the rat. J Neurol Sci 1997;151:141–8.
19. Kohyama K, Matsumoto Y. C protein in the skeletal muscle induces severe autoimmune polymyositis in Lewis rats. J Neuroimmunol 1999;98:130–5.
20. Horai R, Asano M, Sudo K, Kanuka H, Suzuki M, Nishihara M, et al. Production of mice deficient in genes for interleukin (IL)-1α, IL-1β, IL-1α/β, and IL-1 receptor antagonist shows that IL-1β is crucial in turpentine-induced fever development and glucocorticoid secretion. J Exp Med 1998;187:1463–75.
21. Kubo S, Nakayama T, Matsuoka K, Yonekawa H, Karasuyama H. Long term maintenance of IgE-mediated memory in mast cells in the absence of detectable serum IgE. J Immunol 2003;170:775–80.
22. Taniguchi T, Takata M, Ikeda A, Momotani E, Sekikawa K. Failure of germinal center formation and impairment of response to endotoxin in tumor necrosis factor α-deficient mice. Lab Invest 1997;77:647–58.
23. Moll J, Barzaghi P, Lin S, Bezakova G, Lochmuller H, Engvall E, et al. An agrin minigene rescues dystrophic symptoms in a mouse model for congenital muscular dystrophy. Nature 2001;413:302–7.
24. Mogi S, Sakurai J, Kohsaka T, Enomoto S, Yagita H, Okumura K, et al. Tumour rejection by gene transfer of 4-1BB ligand into a CD80+ murine squamous cell carcinoma and the requirements of co-stimulatory molecules on tumour and host cells. Immunology 2000;101:541–7.
25. Lundberg I, Ulfgren AK, Nyberg P, Andersson U, Klareskog L. Cytokine production in muscle tissue of patients with idiopathic inflammatory myopathies. Arthritis Rheum 1997;40:865–74.
26. Kuru S, Inukai A, Liang Y, Doyu M, Takano A, Sobue G. Tumor necrosis factor-α expression in muscles of polymyositis and dermatomyositis. Acta Neuropathol (Berl) 2000;99:585–8.
27. Cherin P, Pelletier S, Teixeira A, Laforet P, Genereau T, Simon A, et al. Results and long-term followup of intravenous immunoglobulin infusions in chronic, refractory polymyositis: an open study with thirty-five adult patients. Arthritis Rheum 2002;46:467–74.
28. Dalakas MC, Illa I, Dambrosia JM, Soueidan SA, Stein DP, Otero C, et al. A controlled trial of high-dose intravenous immune globulin infusions as treatment for dermatomyositis. N Engl J Med 1993;329:1993–2000.
29. Cherin P, Herson S, Wechsler B, Piette JC, Bletry O, Coutellier A, et al. Efficacy of intravenous gammaglobulin therapy in chronic refractory polymyositis and dermatomyositis: an open study with 20 adult patients. Am J Med 1991;91:162–8.
30. Sun D, Whitaker JN, Huang Z, Liu D, Coleclough C, Wekerle H, et al. Myelin antigen-specific CD8+ T cells are encephalitogenic and produce severe disease in C57BL/6 mice. J Immunol 2001; 166:7579–87.
31. Edith M, Janssen EE, Lemmens TW, Urs C, Matthias GH, Stephen PS. CD4+ T cells are required for secondary expansion and memory in CD8+ T lymphocytes. Nature 2003;421:852–6.
32. Matsubara S, Kitaguchi T, Kawata A, Miyamoto K, Yagi H, Hirai S. Experimental allergic myositis in SJL/J mouse: reappraisal of immune reaction based on changes after single immunization. J Neuroimmunol 2001;119:223–30.
33. Eriksson U, Ricci R, Hunziker L, Kurrer MO, Oudit GY, Watts TH, et al. Dendritic cell-induced autoimmune heart failure requires cooperation between adaptive and innate immunity. Nat Med 2003;9:1484–90.
34. Marie I, Hachulla E, Cherin P, Dominique S, Hatron PY, Hellot MF, et al. Interstitial lung disease in polymyositis and dermatomyositis. Arthritis Rheum 2002;47:614–22.
35. Lundberg I, Kratz AK, Alexanderson H, Patarroyo M. Decreased expression of interleukin-1α, interleukin-1β, and cell adhesion

molecules in muscle tissue following corticosteroid treatment in patients with polymyositis and dermatomyositis. Arthritis Rheum 2000;43:336–48.
36. Nakae S, Asano M, Horai R, Sakaguchi N, Iwakura Y. IL-1 enhances T cell-dependent antibody production through induction of CD40 ligand and OX40 on T cells. J Immunol 2001;167:90–7.
37. Saijo S, Asano M, Horai R, Yamamoto H, Iwakura Y. Suppression of autoimmune arthritis in interleukin-1–deficient mice in which T cell activation is impaired due to low levels of CD40 ligand and OX40 expression on T cells. Arthritis Rheum 2002;46:533–44.
38. Eriksson U, Kurrer MO, Sonderegger I, Iezzi G, Tafuri A, Hunziker L, et al. Activation of dendritic cells through the interleukin 1 receptor 1 is critical for the induction of autoimmune myocarditis. J Exp Med 2003;197:323–31.
39. Nagaraju K, Raben N, Merritt G, Loeffler L, Kirk K, Plotz P. A variety of cytokines and immunologically relevant surface molecules are expressed by normal human skeletal muscle cells under proinflammatory stimuli. Clin Exp Immunol 1998;113:407–14.
40. Mantovani A, Bussolino F, Dejana E. Cytokine regulation of endothelial cell function. FASEB J 1992;6:2591–9.
41. Wada H, Saito K, Kanda T, Kobayashi I, Fujii H, Fujigaki S, et al. Tumor necrosis factor-α (TNF-α) plays a protective role in acute viral myocarditis in mice: a study using mice lacking TNF-α. Circulation 2001;103:743–9.
42. Anandacoomarasamy A, Howe G, Manolios N. Advanced refractory polymyositis responding to infliximab. Rheumatology (Oxford) 2005;44:562–3.
43. Campbell IK, O'Donnell K, Lawlor KE, Wicks IP. Severe inflammatory arthritis and lymphadenopathy in the absence of TNF. J Clin Invest 2001;107:1519–27.
44. Sapir T, Blank M, Shoenfeld Y. Immunomodulatory effects of intravenous immunoglobulins as a treatment for autoimmune diseases, cancer, and recurrent pregnancy loss. Ann N Y Acad Sci 2005;1051:743–78.
45. Wada J, Shintani N, Kikutani K, Nakae T, Yamauchi T, Takechi K. Intravenous immunoglobulin prevents experimental autoimmune myositis in SJL mice by reducing anti-myosin antibody and by blocking complement deposition. Clin Exp Immunol 2001; 124:282–9.
46. De Grandmont MJ, Racine C, Roy A, Lemieux R, Neron S. Intravenous immunoglobulins induce the in vitro differentiation of human B lymphocytes and the secretion of IgG. Blood 2003;101: 3065–73.
47. Basta M, Dalakas MC. High-dose intravenous immunoglobulin exerts its beneficial effect in patients with dermatomyositis by blocking endomysial deposition of activated complement fragments. J Clin Invest 1994;94:1729–35.
48. Kaveri S, Vassilev T, Hurez V, Lengagne R, Lefranc C, Cot S, et al. Antibodies to a conserved region of HLA class I molecules, capable of modulating CD8 T cell-mediated function, are present in pooled normal immunoglobulin for therapeutic use. J Clin Invest 1996;97:865–9.
49. Samuelsson A, Towers TL, Ravetch JV. Anti-inflammatory activity of IVIG mediated through the inhibitory Fc receptor. Science 2001;291:484–6.

Available online at www.sciencedirect.com
ScienceDirect
Neuroscience Research 59 (2007) 457–466
Neuroscience Research
www.elsevier.com/locate/neures

Inhibition of glial cell activation ameliorates the severity of experimental autoimmune encephalomyelitis

Xiaoli Guo [a], Kazuaki Nakamura [a], Kuniko Kohyama [b], Chikako Harada [a], Heather A. Behanna [c], D. Martin Watterson [c], Yoh Matsumoto [b], Takayuki Harada [a,*]

[a] *Department of Molecular Neurobiology, Tokyo Metropolitan Institute for Neuroscience, 2-6 Musashidai, Fuchu, Tokyo 183-8526, Japan*
[b] *Department of Molecular Neuropathology, Tokyo Metropolitan Institute for Neuroscience, 2-6 Musashidai, Fuchu, Tokyo 183-8526, Japan*
[c] *Center for Drug Discovery and Chemical Biology, Northwestern University, Chicago, IL 60611, USA*

Received 8 May 2007; accepted 23 August 2007
Available online 30 August 2007

Abstract

Activated microglia and astrocytes have been implicated in the course of multiple sclerosis (MS) and its animal model: experimental autoimmune encephalomyelitis (EAE). MW01-5-188WH is a novel drug that selectively inhibits glial activation in the central nervous system (CNS). We report here that MW01-5-188WH is effective to ameliorate the severity of myelin oligodendrocyte glycoprotein (MOG)-induced EAE. Daily oral administration of MW01-5-188WH at 5 mg/kg body weight reduced the clinical scores of EAE mice while having no influence on the disease incidence or animal mortality. Pathological examination revealed reduced numbers of microglia and astrocytes in the spinal cord of MW01-5-188WH-treated EAE mice. Moreover, MW01-5-188WH suppressed the release of key chemokines, which are involved in MS pathology, from cultured microglia and astrocytes. Taken together, our results indicate that treatments that suppress the activation of microglia and astrocytes should be pursued in future research for their potential as avenues for the treatment of MS.

Keywords: Astrocytes; Chemokines; Experimental autoimmune encephalomyelitis; Glial activation; Microglia; Mouse; MW01-5-188WH; Spinal cord

1. Introduction

Multiple sclerosis (MS) and its animal model, experimental autoimmune encephalomyelitis (EAE), are inflammatory diseases of the central nervous system (CNS) characterized by localized areas of demyelination. The current pathophysiological concept of MS includes genetic and environmental factors as well as a dysfunction in immune regulation. Recent studies have shown the importance of the local environment, especially the activation of glial cells during MS (Ponomarev et al., 2005; Tanuma et al., 2006; Farina et al., 2007). For example, in the gray matter of spinal cord in EAE mice, there are activated astrocytes with increased expression of glial fibrillary acidic protein (GFAP; Liedtke et al., 1998) and activated microglia with increased expression of membrane attack complex-1 (Mac-1; Aharoni et al., 2005). These activated glia produce nitric oxide (NO), proinflammatory cytokines [interferon-γ (IFN-γ), tumor necrosis factor-α (TNF-α), etc.] and chemokines that may contribute to disease progression and related oligodendrocyte cell death (Hisahara et al., 2001; Tanuma et al., 2006; Xu and Drew, 2006). Several chemokines regulated on activation, such as normal T cell expressed and secreted proteins (RANTES), interferon-γ-inducible protein of 10 kDa (IP-10) and monocyte chemoattractant protein (MCP-1), are reported to be upregulated in both MS (Balashov et al., 1999; Van Der Voorn et al., 1999) and EAE (Godiska et al., 1995; Glabinski et al., 1997; Juedes et al., 2000). Consistently, these key chemokines have been linked to the clinical severity of MS and EAE (Godiska et al., 1995; Glabinski et al., 1997; Karpus and Kennedy, 1997; Miyagishi et al., 1997; Balashov et al., 1999; Van Der Voorn et al., 1999; Juedes et al., 2000). Thus, chemokine production can be used as a marker for microglia/astrocyte activation during MS or EAE.

MW01-5-188WH, an orally bioavailable and brain-penetrating small molecule compound that is a novel CNS experimental therapeutic that targets glial activation (Ralay Ranaivo et al., 2006). MW01-5-188WH suppressed the

* Corresponding author. Tel.: +81 42 325 3881; fax: +81 42 321 8678.
E-mail address: harada@tmin.ac.jp (T. Harada).

0168-0102/$ – see front matter
doi:10.1016/j.neures.2007.08.014

lipopolysaccharide (LPS)-induced increase of proinflammatory cytokines, IL-1β and TNF-α, in BV-2 microglia cell line. In addition, MW01-5-188WH effectively suppressed human amyloid-β-induced glial activation and the increased production of proinflammatory cytokines in the hippocampus *in vivo*, with a resultant attenuation of synaptic dysfunction and improvement in hippocampus dependent behavioral deficits (Ralay Ranaivo et al., 2006). Previous studies have shown that other drugs with mechanisms of action that are different from MW01-5-188WH, such as indomethacin and minocycline, also inhibit microglial activation and restore or increase hippocampal neurogenesis (Ekdahl et al., 2003; Monje et al., 2003). However, to our knowledge, there was no report demonstrating an effect on EAE of a drug that inhibits glial activation. Considering the fact that activation of microglia and astrocyte is implicated in the pathogenesis of MS and EAE (Liedtke et al., 1998; Aharoni et al., 2005; Tanuma et al., 2006), it would be of great interest to know whether MW01-5-188WH or future refined analogs of this new class of compounds might be effective for MS. To determine this possibility, we examined the effect of MW01-5-188WH on myelin oligodendrocyte glycoprotein (MOG)-induced EAE mice. Our data showed that MW01-5-188WH ameliorated the severity of EAE by inhibiting the activation of glial cells.

2. Materials and methods

2.1. Mice

Female C57BL/6J mice were obtained from the CLEA Japan (Tokyo, Japan) and maintained at the animal facilities of the Tokyo Metropolitan Institute for Neuroscience. All mice were 6 weeks of age at the time of immunization. Animal treatments were performed in accordance with the Tokyo Metropolitan Institute for Neuroscience *Guidelines for the Care and Use of Animals*.

2.2. EAE induction, MW01-5-188WH administration and clinical scoring

EAE was induced by immunization with rat MOG_{35-55} peptide (MEVGWYRSPFSRVVHLYRNGK) synthesized by an automated peptide synthesizer (model PSSM-8; Shimazu, Kyoto, Japan). Mice were injected subcutaneously at one side of the flanks with 200 μg of rat MOG in complete Freund's adjuvant (Difco Laboratories, Detroit, MI) and 500 μg of *Mycobacterium tuberculosis* H37 RA (Difco). An identical booster was given at the other flank 1 week later. Mice also received intraperitoneal injections of 500 ng pertussis toxin (Seikagaku, Tokyo, Japan) in 200 μl PBS immediately after the first MOG injection and 48 h later. MOG-immunized mice were administrated by oral gavage either MW01-5-188WH (5 mg/kg, treated group) or diluent (10% DMSO, vehicle group) in a 5% acacia suspension once daily according to the following treatment schedules: 1, treatment solely in the induction phase (d0–d12); 2, treatment solely in the effector phase (d13–d30); 3, treatment throughout the whole period of the experiment (d0–d30).

Mice were scored daily for signs of EAE on a scale of 0–9 using the following criteria: 0, no clinical signs; 1, partial tail paralysis; 2, complete tail paralysis; 3, impairment of righting reflex; 4, partial hind limb paralysis; 5, complete hind limb paralysis; 6, partial body paralysis; 7, partial forelimb paralysis; 8, complete forelimb paralysis or moribund; 9, death.

2.3. Spinal cord pathology and immunohistochemistry

On day 30 after immunization, age-matched normal non-immunized mice (normal group), vehicle group and treated group mice were anesthetized with diethylether and perfused transcardially with saline, followed by 4% paraformaldehyde in 0.1 M phosphate buffer containing 0.5% picric acid. The lumbar spinal cords (L1–L3) were removed and postfixed in the same fixative for 2 h at 4 °C and immersed in 30% sucrose in 66 mM phosphate buffer (PB; pH 7.4). Then the spinal cords were embedded in optimal cutting temperature (OCT) compound (Tissue-Tek, Tokyo, Japan) and frozen on dry ice. Cryostat sections (10 μm) were cut coronally and collected on MAS-coated slides (Matsunami, Osaka, Japan). For pathological study, sections were stained with Luxol fast blue (LFB) followed by hematoxylin and eosin (H&E). Immunohistochemistry was performed as previously described (Harada et al., 2006). Briefly, the sections were blocked with phosphate-buffered saline (PBS; pH 7.4) containing 1% normal horse serum and 0.4% Triton-X 100 for 1 h at room temperature. They were incubated overnight at 4 °C with the following primary antibodies: rabbit anti-iba1 (1.0 μg/ml; Harada et al., 2002), rabbit anti-GSTπ (2.0 μg/ml; Medical and Biology Lab, Nagoya, Japan) and mouse anti-GFAP (50 μg/ml; Progen, Heidelberg, Germany), markers for microglia, oligodendrocytes and astrocytes, respectively. The sections were then incubated with Cy-2-conjugated donkey anti-mouse IgG (Jackson ImmunoResearch, West Grove, PA), Cy-2-conjugated donkey anti-rabbit IgG (Jackson ImmunoResearch) or DAKO EnVision (DAKO, Glostrup, Denmark) and DAB substrate kit (DAKO). In some experiments, nuclear staining was performed using Hoechst 33342 (10 μM; Invitrogen, Carlsbad, CA).

2.4. Microscopy and quantification

Stained sections were examined with a microscope (BX51; Olympus, Tokyo, Japan) equipped with Plan Fluor objectives connected to a DP70 camera (Olympus). To quantify immunostaining results, three sections from the spinal cord L1–L3 of each mouse were examined, with three mice per experimental group, for a total of nine sections per experimental group. Digital images from a same area (0.143 mm^2) of the middle region of the ventral horn were captured, and iba1+, GFAP+, GSTπ/Hoechst 33342 double-stained cells in each group were counted from the images. The counting results for each group were averaged and expressed as mean percentage changes compared with age-matched normal group.

2.5. Cell culture

Primary astrocyte and microglia cells were obtained as previously reported (Ohsawa et al., 2007). Cerebral cortices from 1- to 3-day-old C57BL/6 mice were excised, meninges removed and cortices minced into small pieces. Subsequently, the tissue was dissociated by incubation with 0.25% trypsin at 37 °C for 15 min, and the resultant tissue suspension was triturated to yield a single cell suspension. The cells was centrifuged for 5 min at 800 rpm and seeded on a 75 cm^2 tissue culture flask in Dulbecco's Modified Eagle Medium (DMEM) containing 10% fetal bovine serum (FBS). Complete confluence was reached in 7–10 days at 37 °C/5% CO_2. Flasks were then shaken 2 h (150 rpm at 37 °C) in a temperature-controlled shaker to loosen microglia and oligodendrocytes from the more adherent astrocytes. These less adherent cells were plated for 2 h and then lightly shaken to separate oligodendrocytes from the more adherent microglia. Microglia were seeded in 96-well plates (2.5×10^4 cells/well) and incubated 2 h at 37 °C/5% CO_2 before stimulation. After shaking to remove microglia and oligodendrocytes, astrocytes were recovered by trypsinization, seeded in 96-well plates (5×10^4 cells/well) and cultured for 2 days. The above microglia and astrocytes were treated in serum-free media for 16 h either with no stimulus or one of the following three stimuli: LPS (2500 ng/ml), IFN-γ (250 ng/ml) and TNF-α (250 ng/ml), in the presence of diluent or MW01-5-188WH (7.5 and 75 μM for microglia and astrocyte, respectively). Stock solutions (20 mM) of MW01-5-188WHWH are prepared in DMSO. Solutions for cell treatments were prepared by dilution of stock solutions into serum-free media immediately before adding to the cells. Finally, tissue culture supernatants were collected and processed for enzyme-linked immunosorbent assay (ELISA) assays. Control wells contained the same final concentration of DMSO as the compound-containing wells, and the cell viability after treatments was determined by Cell Counting Kit-8 (Dojindo, Kumamoto, Japan).

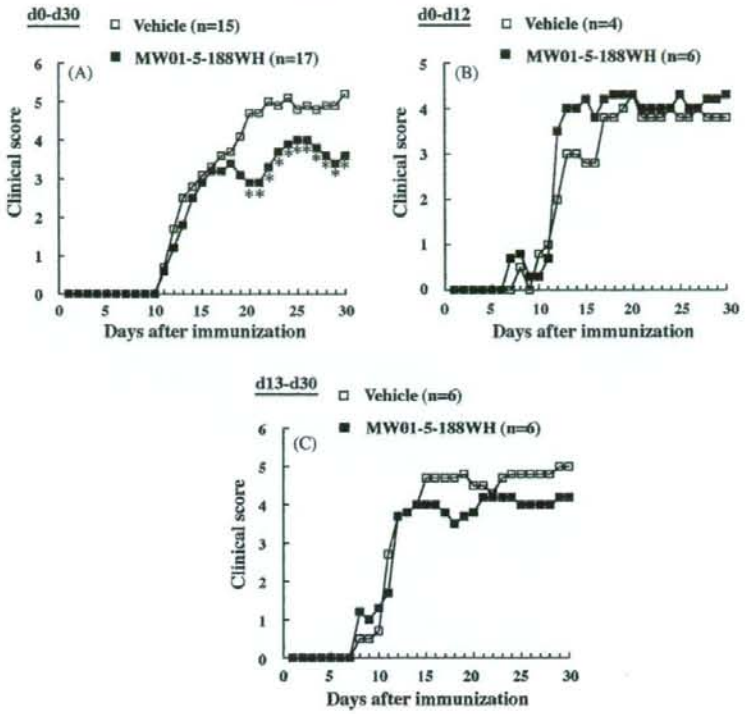

Fig. 1. Effect of MW01-5-188WH on the severity of MOG-induced EAE mice. Mice were orally administrated with MW01-5-188WH (5 mg/kg) or vehicle (10% DMSO in DW) in a 5% acacia suspension in three time frames: the whole experiment period (d0–d30; A), the induction phase (d0–d12; B) and the effector phase (d13–d30; C), and daily mean clinical courses of EAE in mice were shown. When mice were treated for the whole experiment period (A), significant difference in clinical scores between the treated group and vehicle group was found from d20 to d30. When mice were treated only in the induction period (B) or the effector period (C), although no significant differences were found for both two treatments, a tendency of lower scores was found in the effector phase treatment (C). d, days after immunization. $^{*}p < 0.05$.

2.6. Quantitative real-time PCR analysis of chemokines in vivo

A quantitative reverse transcription-polymerase chain reaction assay (qRT-PCR) was performed to measure the expression levels of three chemokine mRNA transcripts (MCP-1, RANTES and IP-10) in the spinal cord as previously reported (Namekata et al., 2006). Total RNA of lumbar spinal cords (L1–L3) freshly dissected from normal, vehicle and MW01-5-188WH-treated EAE mice, which were sacrificed on day 30 after immunization, was extracted with Isogen (Nippon Gene, Tokyo, Japan) according to manufacture's protocol. Resultant RNA was treated with DNase (RQ1 RNase-free DNase, Promega, Madison, WI) and reverse-transcribed with Revertra ace (Toyobo, Osaka, Japan) to obtain cDNA. Quantitative RT-PCR was performed with the ABI 7500 fast real-time PCR system (Applied Biosystems, Foster City, CA) with SYBR Green PCR Master Mix (Applied Biosystems) according to manufacturer's protocol. Thermocycling of each reaction was performed with each primer at a concentration of 100 nM (RANTES: forward primer 5′-GCC CAC GTC AAG GAG TAT TT-3′, reverse primer 5′-TGA CAA ACA CGA CTG CAA GA-3′; IP-10: forward primer 5′-GCT GCA ACT GCA TCC ATA TC-3′, reverse primer 5′-TTT CAT CGT GGC AAT GAT CT-3′; MCP-1: forward primer 5′-AAC TGC ATC TGC CCT AAG GT-3′, reverse primer 5′-ACG GGT CAA CTT CAC ATT CA-3′). The following protocol was used: denaturation program (95 °C for 3 min), followed by the amplification and quantification program (95 °C for 15 s and 60 °C for 30 s) repeated for 50 cycles. The PCR quality and specificity were verified by melting curve analysis. A standard curve of cycle thresholds using serial dilutions of cDNA samples were used to calculate the relative abundance. The difference in the initial amount of total RNA between the samples was normalized in every assay using a glyceraldehyde-3-phosphate

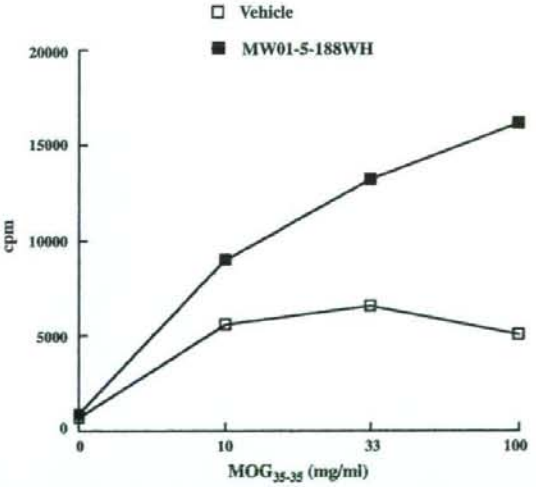

Fig. 2. Effect of MW01-5-188WH on proliferative responses of MOG-specific T cells. Proliferative responses of lymph node cells (3×10^5 cells/well) to MOG at the indicated concentrations were measured 12 days after MOG immunization. No significant difference was found between the two groups.

dehydrogenase (G3PDH) gene expression as an internal standard (forward primer 5′-TGC ACC ACC AAC TGC TTA G-3′, reverse primer 5′-GGA TGC AGG GAT GAT GTT C-3′).

2.7. ELISA

Chemokine (RANTES, MCP-1, IP-10) levels in cell culture media were determined by ELISA according to the manufacturer's instructions (BioSource, Camarillo, CA; R&D Systems, Minneapolis, MN). Optical densities were measured using a Model 550 microplate reader (Bio-Rad, Hercules, CA) at 450 nm. Chemokine concentrations in media were calculated from standards containing known concentrations of the proteins.

2.8. Proliferation assay

Proliferative responses of lymph node (LN) cells from vehicle and MW01-5-188WH-treated mice were assayed in microtiter wells by uptake of [^{3}H]thymidine in accord with the procedure reported elsewhere (Arimoto et al., 2000). After washing with PBS, LN cells (3×10^5 cells/well) were cultured with given concentrations of MOG_{35-55} for 3 days, with the last 18 h in the presence of

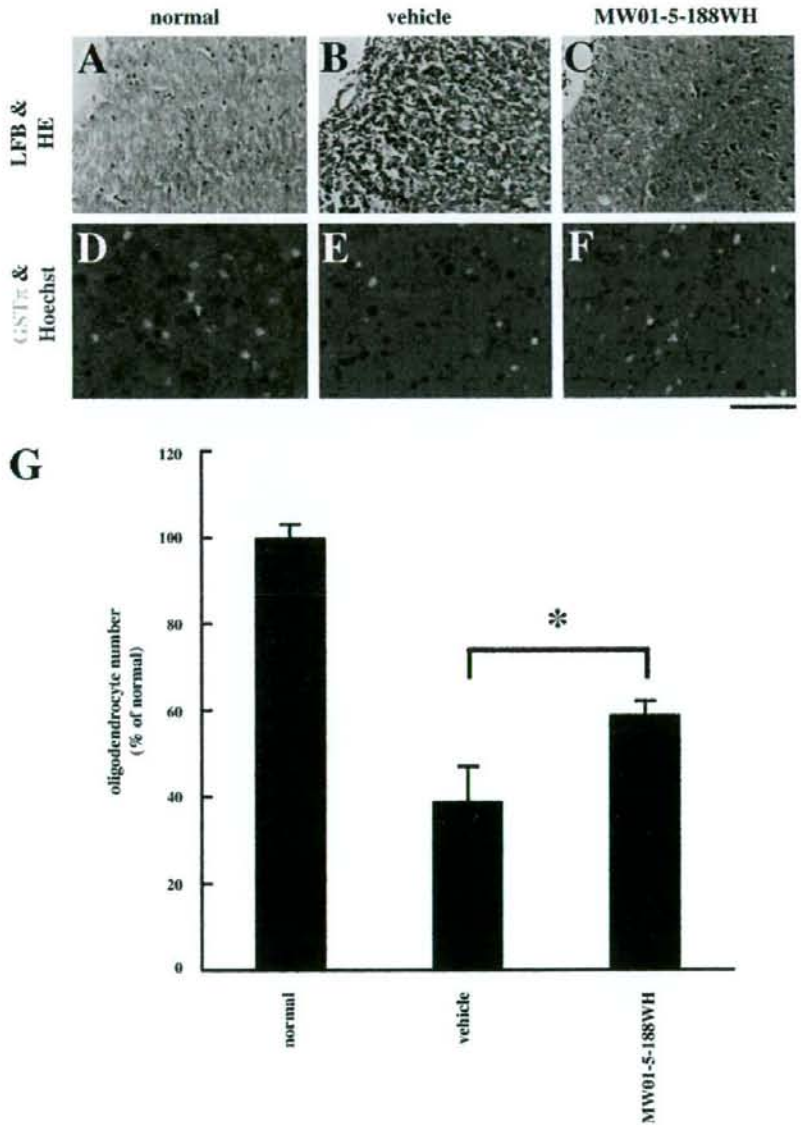

Fig. 3. Effect of MW01-5-188WH on the extent of demyelination and oligodendrocyte cell death in EAE mice. (A–C) Representative LFB- and H&E-stained region of lateral funiculus of spinal cords from non-EAE normal (A), vehicle (B)- and MW01-5-188WH (C)-treated EAE mice. (D–F) GSTπ and Hoechst33342 double-stained region of gray matter of spinal cords from non-EAE normal (D), vehicle (E)- and MW01-5-188WH (F)-treated EAE mice. (G) Quantification of oligodendrocytes presented as percentage of normal. Results of three independent animals are presented as mean ± S.E.M. Note the increased oligodendrocyte number after MW01-5-188WH treatment. Scale bar: 100 μm in (A–C) and 70 μm in (D–F). $^*p < 0.05$.

0.5 μCi [^{3}H]thymidine (GE Healthcare Bioscience, Tokyo, Japan). The cells were harvested on glass-fiber filters, and the label uptake was determined using standard liquid scintillation techniques.

2.9. Statistics

Data are presented as mean ± S.E.M. except otherwise noted. Student's *t*-test was used to estimate the significance of difference in results. Statistical significance was accepted at $p < 0.05$.

3. Results

3.1. Effect of MW01-5-188WH on clinical course of EAE

We examined the effect of MW01-5-188WH by daily oral administration from 0 to 30 days after the disease induction (d0–d30). Clinical signs of EAE in vehicle and MW01-5-188WH-treated groups developed 13.5 ± 0.8 ($n = 15$) and 12.6 ± 0.4 ($n = 17$) days after the first MOG immunization, and no significant difference was found between the groups ($p = 0.168$, Fig. 1A). On the other hand, the daily mean clinical scores were lower in the MW01-5-188WH-treated group compared to the vehicle group, but significant differences were first detected at d20 ($p = 0.009$). The mean clinical scores of the vehicle and treated groups on d30 were 5.2 ± 0.4 and 3.6 ± 0.5, respectively ($p = 0.012$).

The initial immunopathological event of EAE starts when auto-reactive T cells in the systemic immune compartment are activated through the recognition of their specific antigen (induction phase), which finally leads to a stimulation of microglia/astrocytes in the central nervous system (effector phase) (Magnus and Rao, 2005). So, we next examined the effect of MW01-5-188WH on the antigen-specific T cell proliferation and representative data from one mouse of each group was shown in Fig. 2. Freshly isolated T cells from the drug- and vehicle-treated mice both responded to MOG at any of the concentrations tested, but no significant difference was found between the two groups. This result indicates that MW01-5-188WH does not modulate the immune response in EAE mice at a dose that alters clinical presentation.

We also examined the effect of MW01-5-188WH in two different time frames, namely in the induction phase (d0–d12) and in the effector phase (d13–d30). When EAE mice were treated solely in the induction phase, no significant difference of clinical scores was found in vehicle and MW01-5-188WH-treated groups (Fig. 1B). When mice were treated in the effector period, although no significant differences was detected, a tendency of lower scores was found in the MW01-5-188WH-treated group (Fig. 1C). These results suggest that MW01-5-188WH ameliorates the severity of MOG-induced EAE by mainly inhibiting the glial activation in the effector phase.

3.2. Effect of MW01-5-188WH on pathology of EAE

We next examined the histological basis of MW01-5-188WH's protective effect on the EAE clinical score. LFB and H&E staining showed that MOG immunization induced inflammation and demyelination in the mouse spinal cord (Fig. 3A–C). Numerous inflammatory cell infiltrates were observed in the white matter of the spinal cord in the vehicle group (purple dots in Fig. 3B) relative to that in the normal group (Fig. 3A). And areas containing myelin were decreased in the vehicle group compared with that in the normal group (blue areas in Fig. 3A and B). MW01-5-188WH treatment significantly reduced inflammation and demyelination (Fig. 3C). In addition, this improvement was accompanied by an increased survival rate of oligodendrocytes in the treated group (Fig. 3F) compared with the vehicle group (Fig. 3E). Quantitative analysis revealed that the percentage of surviving GSTπ-positive oligodendrocytes increased from 39 ± 7% in the vehicle group to 60 ± 3% in the treated group ($p < 0.05$, Fig. 3G). These results suggest that MW01-5-188WH improved pathology of MOG-induced EAE by suppressing

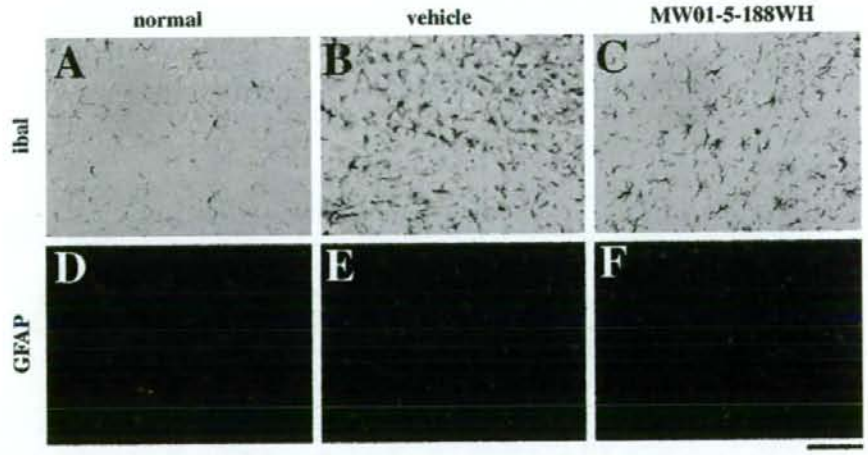

Fig. 4. Effect of MW01-5-188WH on glial activation in EAE mice. Representative iba1 (A–C)- and GFAP (D–F)-stained region of gray matter of spinal cords from non-EAE normal (A and D), vehicle (B and E)- and MW01-5-188WH (C and F)-treated EAE mice. Scale bar: 50 μm.

inflammation, demyelination and depletion of oligodendrocytes.

3.3. Effect of MW01-5-188WH on the activity of microglia and astrocytes in EAE

Microglia and astrocytes in the spinal cord are activated upon EAE induction (Liedtke et al., 1998; Aharoni et al., 2005). We determined these phenomena in our EAE model, and found that the number of iba1-positive microglia was increased (Fig. 4B) compared with the normal group (Fig. 4A). Since MW01-5-188WH selectively inhibits the activation of glial cells (Ralay Ranaivo et al., 2006), we next examined its effect on microglial activation in our EAE model. Daily oral administration of MW01-5-188WH decreased the number of microglia from 650 ± 7% in the vehicle group to 340 ± 13% ($p = 0.003$, Fig. 5A). Activated form of microglia was also decreased by this treatment (Fig. 4C). Similarly, the number of GFAP-positive astrocytes was increased upon EAE induction (Fig. 4E) compared with that in the normal group (Fig. 4D). MW01-5-188WH treatment also suppressed the increase from 242 ± 7% in the vehicle group to 158 ± 2% in the treated group ($p = 0.002$, Figs. 4F and 5B). Taken together, these results suggest that MW01-5-188WH treatment had inhibitory effects on the activity of microglia and astrocytes in EAE.

3.4. Effect of MW01-5-188WH on chemokine production in vivo and in vitro

Activated microglia and astrocytes produce various chemokines such as RANTES, IP-10 and MCP-1 that have been shown to contribute to the disease progression of MS and EAE (Balashov et al., 1999; Juedes et al., 2000). To determine whether MW01-5-188WH suppresses the *in vivo* increase in the concentration of these three chemokines, we first investigated the chemokine production levels in the spinal cord. When EAE was induced, all three chemokines' mRNA transcripts in the spinal cord were increased as shown in Fig. 6. While there was a tendency of lower expression levels of three chemokines in MW01-5-188WH-treated mice, no significant difference was found compared with the vehicle group. Since this method may mask the effect of MW01-5-188WH on chemokine productions in glial cells, we next examined its effect directly on cultured microglia and astrocytes. We prepared primary cultured microglia and astocytes, and stimulated them with LPS, IFN-γ or TNF-α in the presence or absence of compound. Release of RANTES was increased by all three stimuli and MW01-5-188WH significantly suppressed its release from both microglia (Fig. 7A) and astrocytes (Fig. 8A). MW01-5-188WH also suppressed the release of IP-10 from astrocytes (Fig. 8B), but it was effective only when stimulated by TNF-α in microglia (Fig. 7B). Similar variance was observed for MCP-1. MW01-5-188WH suppressed its release when stimulated by LPS or IFN-γ in microglia (Fig. 7C), whereas it was effective for LPS and TNF-α in astrocytes (Fig. 8C). MW01-5-188WH and all three stimuli did not kill microglia and astrocytes (data not shown), indicating that the suppression of chemokine release by MW01-5-188WH was not due to its effect on cell viability. These results suggest that MW01-5-188WH, at least partially, suppresses the number and activity of microglia and astrocytes, which may lead to the improvement of clinical signs and pathology in EAE.

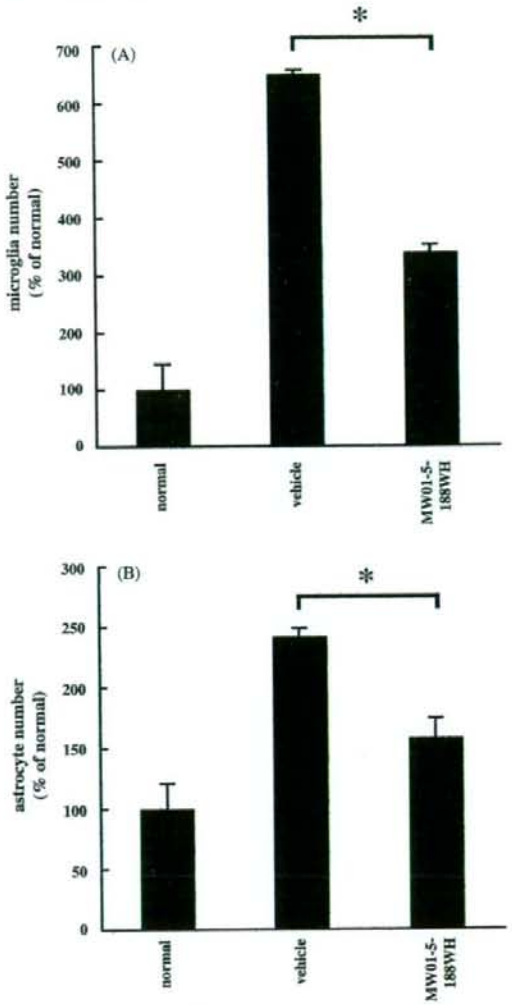

Fig. 5. Effect of MW01-5-188WH on glial cell number in EAE mice. Quantitative analysis of cell number in microglia (A) and astrocytes (B) in EAE mice presented as percentage of normal. Results of three independent experiments are presented as mean ± S.E.M. Note the decreased number in microglia and astrocytes after MW01-5-188WH treatment. $^{*}p < 0.05$.

4. Discussion

The initial immunopathological event of EAE and MS starts when auto-reactive T cells in the systemic immune compartment are activated and cross the blood–brain barrier and re-encounter their antigen (Magnus and Rao, 2005). This

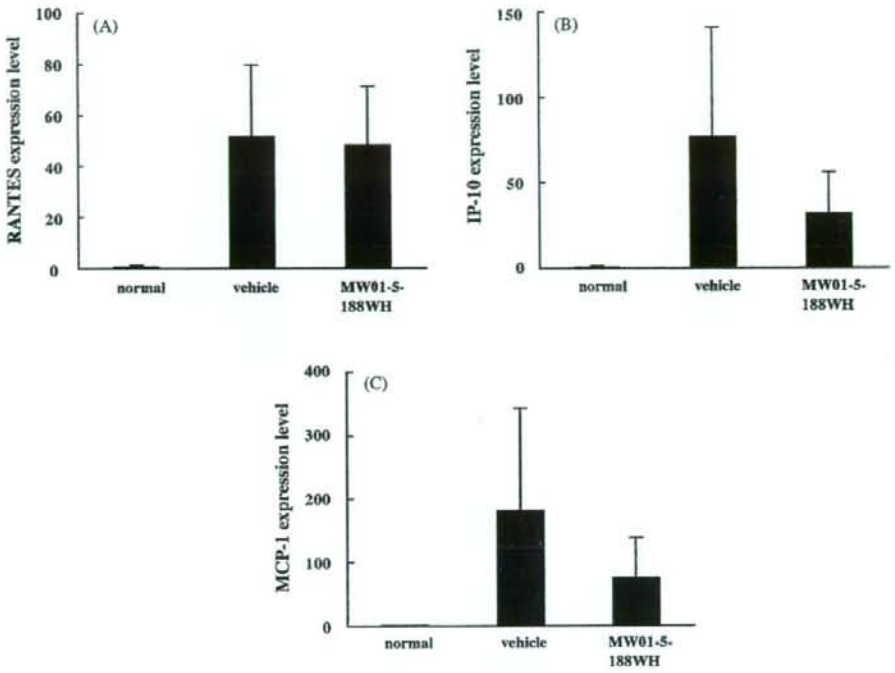

Fig. 6. Effect of MW01-5-188WH on chemokine production *in vivo*. mRNA expression levels of RANTES (A), IP-10 (B) and MCP-1 (C) in the spinal cords dissected from different treatment groups were measured by quantitative RT-PCR. Data in vehicle- and MW01-5-188WH-treated groups were normalized according to those in the normal group.

encounter leads to a reactivation and expansion of the autoreactive T cells that in turn stimulates microglia/astrocytes to increase their activities, to release more proinflammatory cytokines and chemokines. The release of these mediators induces demyelination and axonal degeneration. Based on the fact that MS and EAE are inflammatory diseases associated with activated glial cells, interventions targeting the immune response or the reactive glia seem to be possible. Over the last decades, changing the direct immune response has been the main strategy of multiple studies (Matsumoto and Fujiwara, 1993; Aharoni et al., 2005). And the current treatment of MS is based on immune modulators such as glatiramer acetate (Neuhaus et al., 2000; Kieseier and Hartung, 2003) or immune suppressors such as mitoxantrone (Hartung et al., 2002). However, almost no pharmacological study has been done on the treatment of EAE with reactive glial cells as the main targets. In the present study, we focused on a therapeutic strategy on targeting reactive glia using a novel CNS drug that has never been applied for EAE. We tested whether the administration of MW01-5-188WH is effective for the treatment of EAE.

MW01-5-188WH is a novel CNS drug designed to target glial activation (Ralay Ranaivo et al., 2006). Our *in vivo* results showed that the oral administration of MW01-5-188WH reduced both the clinical and pathological severities of EAE. MW01-5-188WH has been demonstrated *in vivo* to effectively suppress human amyloid-β-induced glial activation and decrease the production of proinflammatory cytokines in the hippocampus. In our present study, consistent with previous studies (Liedtke et al., 1998; Aharoni et al., 2005), activation of microglia and astrocytes was observed in the spinal cord of EAE mice. MW01-5-188WH administration at 5 mg/kg inhibited this glial activation, and resulted in the improvement of clinical scores and a partial rescue of oligodendrocytes from cell death. On the other hand, MW01-5-188WH administration at this low dose did not alter the proliferation response of T cells from mice immunized with MOG. Furthermore, the drug administered during the induction phase had no effect on the severity of EAE. Thus, this drug does not seem to have major effect on the immune system at an effective dose that brings about attenuation of glial activation. Certainly, no significant differences were found when MW01-5-188WH was administrated in the effector phase (d13–d30) solely, but glial activation might have been partially induced in the "initiation phase", especially during d10–d12, in animals demonstrating EAE signs before d13 (Fig. 1C). Another concern is that selectivity of pharmacological effects on activation of T cells or B-cells over a range of doses remains to be determined for the drug candidate compound MW01-5-188WH. Craft et al. (2006) previously showed in early integrative chemical biology studies that the bioavailable compound MW01-070C could suppresses CNS inflammatory responses at doses that did not suppress peripheral immune responses including T cell and B cell activation. Taken in their entirety, the available

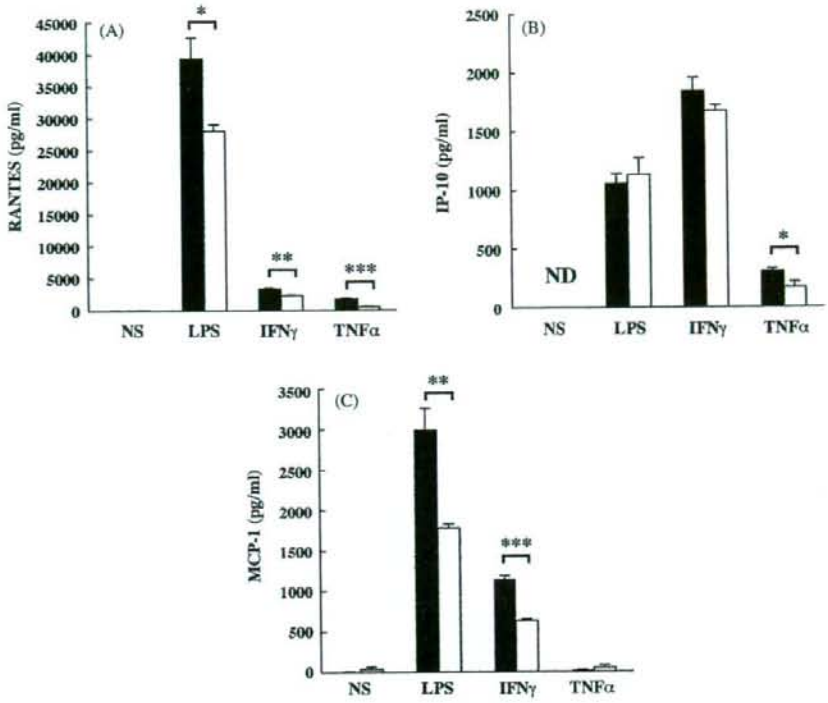

Fig. 7. Effect of MW01-5-188WH on chemokine production by microglia. Cells were treated for 16 h with or without 7.5 μM MW01-5-188WH under non-stimulation, or stimulation with LPS (2500 ng/ml), IFN-γ (250 ng/ml) or TNF-α (250 ng/ml). RANTES (A), IP-10 (B) and MCP-1 (C) levels were determined in culture medium by ELISA. Values represent the mean ± S.E.M. for a representative experiment run in quadruplicate. Note the decreased chemokine production by microglia after MW01-5-188WH treatment. NS, no stimulus; ND, non-detectable. $^{*}p < 0.05$, $^{**}p < 0.01$, $^{***}p < 0.001$.

data provide a proof-of-concept that it is possible to selectively restore excessive proinflammatory responses in the CNS back towards homeostasis at doses of a peripherally administered compound that do not suppress systemic immune and inflammatory responses. Thus, our results support the concept that glial cells are possible therapeutic targets for MS (Heppner et al., 2005; Tanuma et al., 2006) as well as other neurodegenerative disorders (Harada et al., 2000, 2002; Farina et al., 2007).

Oligodendrocyte cell death occurs in the course of EAE. The factors mediating the death of oligodendrocytes can be summarized into two categories. One is the endogenous factors such as processed caspase-11 and activated caspase-3, leading to cell death via specific pathways (Hisahara et al., 2001). The other is the cytotoxic cytokines that are released from activated microglia and astrocytes, which may activate caspase cascades through their receptors in oligodendrocytes (Selmaj et al., 1991; Louis et al., 1993; Vartanian et al., 1995; Hisahara et al., 1997, 2001). MW01-5-188WH has been shown to suppress the release of proinflammatory cytokines such as IL-1β and TNF-α from microglia (Ralay Ranaivo et al., 2006). In addition, this drug significantly inhibited the release of RANTES, IP-10 and MCP-1 from primary cultured microglia and astrocytes. It is well known that chemokines are essential for inflammatory responses because they recruit specific subsets of leukocytes and monocytes into tissues (Luster, 1998; Zlotnik and Yoshie, 2000). For example, IP-10 is a strong candidate for recruiting T cell response and activated T cells express IP-10 receptor (Dufour et al., 2002; Christensen et al., 2004). $CD4^{+}$ and $CD8^{+}$ T cells and monocytes express RANTES receptor (Sorensen et al., 1999) and MCP-1 acts toward monocytes and T cells via type 2 CC chemokine receptor (CCR2; Sorensen et al., 1999). Therefore, MW01-5-188WH seems to reduce oligodendrocyte cell death, at least partly through the attenuation of microglia and astrocyte activation, which may subsequently reduce the release of key chemokines, infiltration of inflammatory cells, and spinal cord damage in EAE mice. Although further studies are needed, interfering with the interactions between glial cells might be a potential therapeutic strategy for the treatment of MS/EAE.

Acknowledgements

We thank Drs. K. Ohsawa, Y. Nakamura, and S. Kohsaka for their advice on microglia cell culture. This work was supported by grants from the Ministry of Education, Culture, Sports, Science and Technology of Japan (CH and TH), Naito Foundation and Uehara Memorial Foundation (TH). CH was supported by the Japan Society for the Promotion of Science for Young Scientists.

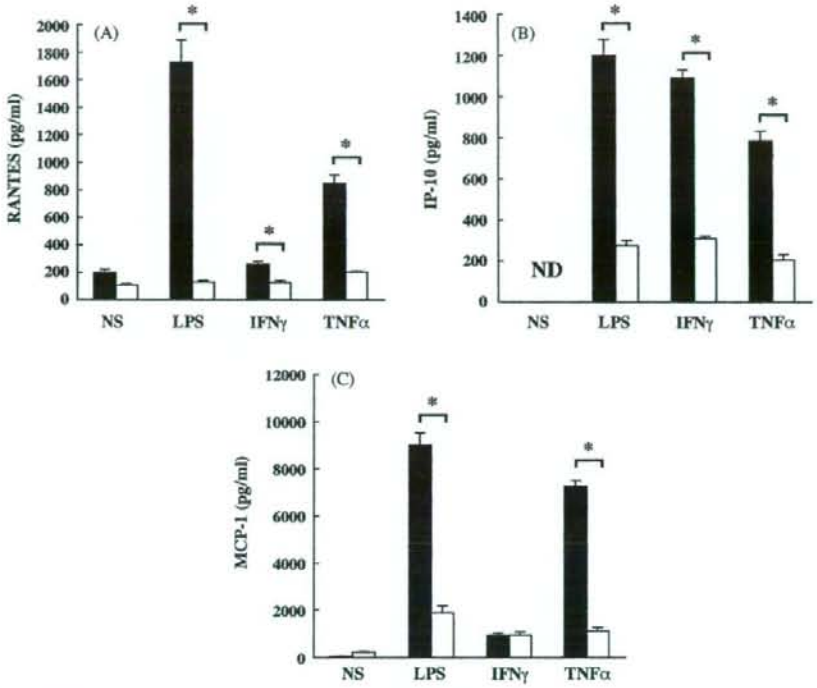

Fig. 8. Effect of MW01-5-188WH on chemokine production by astrocytes. Cells were treated for 16 h with or without 75 μM MW01-5-188WH under non-stimulation, or stimulation with LPS (2500 ng/ml), IFN-γ (250 ng/ml) or TNF-α (250 ng/ml). RANTES (A), IP-10 (B) and MCP-1 (C) levels were determined in culture medium by ELISA. Values represent the mean ± S.E.M. for a representative experiment run in quadruplicate. Note the decreased chemokine production by astrocytes after MW01-5-188WH treatment. NS, no stimulus; ND, non-detectable. $^{*}p < 0.001$.

References

Aharoni, R., Arnon, R., Eilam, R., 2005. Neurogenesis and neuroprotection induced by peripheral immunomodulatory treatment of experimental autoimmune encephalomyelitits. J. Neurosci. 25, 8217–8228.

Arimoto, H., Tanuma, N., Jee, Y., Miyazawa, T., Shima, K., Matsumoto, Y., 2000. Analysis of experimental autoimmune encephalomyelisis induced in F344 rats by pertussis toxin administration. J. Neuroimmunol. 104, 15–21.

Balashov, K., Rottman, J., Weiner, H., Hancock, W., 1999. CCR5+ and CXCR3+ T cells are increased in multiple sclerosis and their lignads MIP-1 and IP-10 are expressed in demyelinating braining lesions. Proc. Natl. Acad. Sci. U.S.A. 96, 6873–6878.

Christensen, J.E., Nansen, A., Moos, T., Lu, B., Gerard, C., Christensen, J.P., Thomsen, A.R., 2004. Efficient T-cell surveillance of the CNS requires expression of the CXC chemokine receptor 3. J. Neurosci. 24, 4849–4858.

Craft, J.M., Watterson, D.M., Van Eldik, L.J., 2006. Human amyloid β-induced neuroinflammation is an early event in neurodegeneration. Glia 53, 484–490.

Dufour, J.H., Dziejman, M., Liu, M.T., Leung, J.H., Lane, T.E., Luster, A.D., 2002. IFN-γ-inducible protein 10 (IP-10; CXCL10)-deficient mice reveal a role for IP-10 in effector T cell generation and trafficking. J. Immunol. 168, 3195–3204.

Ekdahl, C.T., Claasen, J.H., Bonde, S., Kokaia, Z., Lindvall, O., 2003. Inflammation is detrimental for neurogenesis in adult brain. Proc. Natl. Acad. Sci. U.S.A. 100, 13632–13637.

Farina, C., Aloisi, F., Meinl, E., 2007. Astrocytes are active players in cerebral innate immunity. Trends Immunol. 28, 138–145.

Glabinski, A.R., Tani, M., Strieter, R.M., Tuohy, V.K., Ransohoff, R.M., 1997. Synchronous synthesis of alpha- and beta-chemokines by cells of diverse lineage in the central nervous system of mice with relapses of chronic experimental autoimmune encephalomyelitis. Am. J. Pathol. 150, 617–630.

Godiska, R., Chantry, D., Dietsch, G.N., Gray, P.W., 1995. Chemokine expression in murine experimental allergic encephalomyelitis. J. Neuroimmunol. 58, 167–176.

Harada, C., Nakamura, K., Namekata, K., Okumura, A., Mitamura, Y., Iizuka, Y., Kashiwagi, K., Yoshida, K., Ohno, S., Matsuzawa, A., Tanaka, K., Ichijo, H., Harada, T., 2006. Role of apoptosis signal-regulating kinase 1 in stress-induced neural cell apoptosis *in vivo*. Am. J. Pathol. 168, 261–269.

Harada, T., Harada, C., Kohsaka, S., Wada, E., Yoshida, K., Ohno, S., Mamada, H., Tanaka, K., Parada, L.F., Wada, K., 2002. Microglia–Muller glia cell interactions control neurotrophic factor production during light-induced retinal degeneration. J. Neurosci. 22, 9228–9236.

Harada, T., Harada, C., Nakayama, N., Okuyama, S., Yoshida, K., Kohsaka, S., Matsuda, H., Wada, K., 2000. Modification of glial–neuronal cell interactions prevents photoreceptor apoptosis during light-induced retinal degeneration. Neuron 26, 533–541.

Hartung, H.P., Gonsette, R., Konig, N., Kwiecinski, H., Guseo, A., Morrissey, S.P., Karpf, H., Zwingers, T., 2002. Mitoxantrone in progressive multiple sclerosis: a placebo-controlled, double-blind, randomized, multicentre trial. Lancet 360, 2018–2025.

Heppner, F.L., Greter, M., Marino, D., Falsig, J., Raivich, G., Hovelmeyer, N., Waisman, A., Rulicke, T., Prinze, M., Priller, J., Becher, B., Aguzzi, A., 2005. Experimental autoimmune encephalomyelitis repressed by microglial paralysis. Nat. Med. 11, 146–152.

Hisahara, S., Shoji, S., Okano, H., Miura, M., 1997. ICE/CED-3 family executes oligodendrocyte apoptosis by tumor necrosis factor. J. Neurochem. 69, 10–20.

Hisahara, S., Yuan, J., Momoi, T., Okano, H., Miura, M., 2001. Caspase-11 mediates oligodendrocyte cell death and pathogenesis of autommune-mediated demyelination. J. Exp. Med. 193, 111–122.

Juedes, A.E., Hjelmstrom, P., Bergman, C.M., Neild, A.L., Ruddle, N.H., 2000. Kinetics and cellular origin of cytokines in the central nervous system:

insight into mechanisms of myelin oligodendrocyte glycoprotein-induced experimental autoimmune encephalomyelitis. J. Immunol. 164, 419–426.
Karpus, W.J., Kennedy, K.J., 1997. MIP-1alpha and MCP-1 differentially regulate acute and relapsing autoimmune encephalomyelitis as well as Th1/Th2 lymphocyte differentiation. J. Leukoc. Biol. 62, 681–687.
Kieseier, B.C., Hartung, H.P., 2003. Current disease-modifying therapies in multiple sclerosis. Semin. Neurol. 23, 133–146.
Liedtke, W., Edelmann, W., Chiu, F.C., Kucherlapati, R., Raine, C.S., 1998. Experimental autoimmune encephalomyelitis in mice lacking glial fibrillary acidic protein is characterized by a more severe clinical course and an infiltrative central nervous system lesion. Am. J. Pathol. 152, 251–259.
Louis, J.C., Magal, E., Takayama, S., Varon, S., 1993. CNTF protection of oligodendrocytes against natural and tumor necrosis factor-induced death. Science 259, 689–692.
Luster, A.D., 1998. Chemokines-chemotactic cytokines that mediate inflammation. N. Engl. J. Med. 338, 436–445.
Magnus, T., Rao, M.S., 2005. Neural stem cells in inflammatory CNS diseases: mechanisms and therapy. J. Cell. Mol. Med. 9, 303–319.
Matsumoto, Y., Fujiwara, M., 1993. Immunomodulation of experimental autoimmune encephalomyelitis by Staphylococcal enterotoxin D. Cell. Immunol. 149, 268–278.
Miyagishi, R., Kikuchi, S., Takayama, C., Inoue, Y., Tashiro, K., 1997. Identification of cell types producing RANTES. MIP-1α and MIP-1β in rat experimental autoimmune encephalomyelitis by in situ hybridization. J. Neuroimmunol. 77, 17–26.
Monje, M.L., Toda, H., Palmer, T.D., 2003. Inflammatory blockade restores adult hippocampal neurogenesis. Science 302, 1760–1765.
Namekata, K., Okumura, A., Harada, C., Nakamura, K., Yoshida, H., Harada, T., 2006. Effect of photoreceptor degeneration on RNA splicing and expression of AMPA receptors. Mol. Vis. 12, 1586–1593.
Neuhaus, O., Farina, C., Yassouridis, A., Wiendl, H., Then, B.F., Dose, T., Wekerle, H., Hohlfeld, R., 2000. Multiple sclerosis: comparison of copolymer-1-reactive T cell lines from treated and untreated subjects reveals cytokine shift from T helper 1 to T helper 2 cells. Proc. Natl. Acad. Sci. U.S.A. 97, 7452–7457.
Ohsawa, K., Irino, Y., Nakamura, Y., Akazawa, C., Inoue, K., Kohsaka, S., 2007. Involvement of P2X4 and P2Y12 receptors in ATP-induced microglial chemotaxis. Glia 55, 604–616.
Ponomarev, E.D., Shriver, L.P., Maresz, K., Dittel, B.N., 2005. Microglial cell activation and proliferation precedes the onset of CNS autoimmunity. J. Neurosci. Res. 81, 374–389.
Ralay Ranaivo, H., Craft, J.M., Hu, W., Guo, L., Wing, L.K., Van Eldik, L.J., Watterson, D.M., 2006. Glia as a therapeutic target: selective suppression of human amyloid-β-induced upregulation of brain proinflammatory cytokine production attenuates neurodegeneration. J. Neurosci. 26, 662–670.
Selmaj, K., Raine, C.S., Farooq, M., Norton, W.T., Brosnan, C.F., 1991. Cytokine cytotoxicity against oligodendrocytes. Apoptosis induced by lymphotoxin. J. Immunol. 147, 1522–1529.
Sorensen, T.L., Tani, M., Jensen, J., Pierce, V., Lucchinetti, C., Folcik, V.A., Qin, S., Rottman, J., Sellebjerg, F., Strieter, R.M., Frederiksen, J.L., Ransohoff, R.M., 1999. Expression of specific chemokines and chemokine receptors in the central nervous system of multiple sclerosis patients. J. Clin. Invest. 103, 807–815.
Tanuma, N., Sakuma, H., Sasaki, A., Matsumoto, Y., 2006. Chemokine expression by astrocytes plays a role in microglia/macrophage activation and subsequent neurodegeneration in secondary progressive multiple sclerosis. Acta Neuropathol. 112, 195–204.
Van Der Voorn, P., Tekstra, J., Beelen, R.H., Tensen, C.P., Van Der Valk, P., De Groot, C.J., 1999. Expression of MCP-1 by reactive astrocytes in demyelinating multiple sclerosis lesions. Am. J. Pathol. 154, 45–51.
Vartanian, T., Li, Y., Zhao, M., Stefansson, K., 1995. Interferon-induced oligodendrocyte cell death: implications for the pathogenesis of multiple sclerosis. Mol. Med. 1, 732–743.
Xu, J., Drew, P., 2006. 9-cis-Retinoic acid suppresses inflammatory responses of microglia and astrocytes. J. Neuroimmunol. 171, 135–144.
Zlotnik, A., Yoshie, O., 2000. Chemokines: a new classification system and their role in immunity. Immunity 12, 121–127.